Fate and availability of phosphorus from bone char with and without sulfur modification in soil size fractions after five-year field fertilizations

Yunsheng Jia[1*], Nina Siebers[1], Kerstin Panten[2], Jens Kruse[1,3]

[1]Institute of Bio- and Geosciences, Agrosphere (IBG-3), Forschungszentrum Jülich GmbH, Wilhelm Johnen Straße, 52425 Jülich, Germany

[2]Julius Kühn Institute (JKI), Federal Research Centre for Cultivated Plants, Institute for Crop and Soil Science, Bundesallee 58, 38116 Braunschweig, Germany

[3]Institute of Crop Science and Resource Conservation (INRES), Soil Science and Soil Ecology, University of Bonn, Nussallee 13, 53115 Bonn, Germany

[*] Corresponding author.

E-mail address: yunshengjia@163.com

Abstract

The agronomic value of fertilizer phosphorus (P) in the soil is determined by how it is incorporated and released during aggregate formation and breakdown. These processes play a vital role in P accessibility, storage, and cycling. Bone char (BC) is a promising substitute for phosphorus fertilizer. Its low P solubility can be increased by modifying the BC surface with elemental sulfur (BC^{plus}), although the fate of BC-based P within soil aggregates have not yet been tested under field conditions. In this study, soil samples were taken from a five-year field experiment (2013-2018) to track the fate of BC and BC^{plus} P. These samples were compared to triple superphosphate (TSP) and a control without additional P (No-P) in different soil P pools within soil aggregates in severely P deficient vs. sufficiently P fertilized Cambisol. Soil aggregate distributions were assessed after wet-sieving, centrifugation, and tangential flow filtration to separate small macroaggregates (250 to 2000 µm, SMaA), large microaggregates (53 to 250 µm, LMiA), small microaggregates (1 to 53 µm, SMiA), and composite building units (< 1 µm, BU). Soil P status was assessed after sequential extraction (Hedley scheme). We found that the mass proportions of soil size fractions decreased in the order of SMiA > LMiA ≈ SMaA > BU. The addition of 45 kg P ha^{-1} $year^{-1}$ using different fertilizers significantly increased the mass proportion of LMiA from 7 to 22% in comparison to the No-P. This was likely due to stimulated plant growth after fertilization and thus introduction of organic binding agents which increased soil aggregation. The addition of BC and BC^{plus} showed nearly no significant effect when compared to No-P on soil P pools. However, sulfur modification of BC resulted in higher labile P which was comparable to that found in TSP. Therefore, we conclude that BC^{plus} behaves similarly to TSP, without any additional positive or detrimental effects on P status. This lends support for the use of BC wastes as a possible substitute for TSP, which would represent a move towards more sustainable agriculture with more closed P cycles.

Keywords

Sulfur modified bone char; Hedley fractionation; P fertilizer substitute; soil aggregates; P pools

1. Introduction

Phosphorus (P) plays a vital role in supporting soil fertility and food production (Holford, 1997; Roberts and Johnston, 2015; Scholz et al., 2013; Vance et al., 2003). However, there are considerable uncertainties about how long the finite rock phosphate (RP) reserves can cover global need (Cordell et al., 2009; Obersteiner et al., 2013). There is further concern about contamination with cadmium (Cd) and uranium (U), as well as the globally uneven distribution of the remaining P reservoirs (Desmidt et al., 2015; Obersteiner et al., 2013; Scholz et al., 2013). These factors drive current research on novel P sources and approaches for sustainable agricultural P management.

Recent studies have shown that bone char (BC) based materials is a promising recycled P fertilizer (Glaesner et al., 2019; Kruse et al., 2022; Morshedizad and Leinweber, 2017; Morshedizad et al., 2018; Siebers et al., 2014; Siebers et al., 2013; Siebers and Leinweber, 2013; Zimmer et al., 2018; Zwetsloot et al., 2016). Bone char is produced from the pyrolysis of animal bone chips, which usually are regarded as waste in slaughterhouses (Leinweber et al., 2019; Zimmer et al., 2018). It is completely free of soil contaminants, such as Cd and U, and in addition to calcium (Ca) and magnesium (Mg), contains considerable amounts of P (roughly 130 to 150 g P kg^{-1}), mainly in the form of hydroxyapatite (Leinweber et al., 2019; Siebers and Leinweber, 2013). Furthermore, due to its biological origin and associated lower crystallinity this hydroxyapatite is more soluble than geological apatite (Zwetsloot et al., 2015). Plant availability and P release kinetics of BC have been primarily studied in lab or pot experiments (Leinweber et al., 2019; Siebers et al., 2014; Zwetsloot et al., 2016), but recently have also begun to be studied in the field (Panten and Leinweber, 2020). The major factors controlling the dissolution of both BC and RP are soil pH and sinks of soil P and Ca (Warren et al., 2008). It has been shown that P dissolution from BC is generally slower than that from commercially available and highly soluble P fertilizers (Siebers and Leinweber, 2013) and althrough higher soil acidity can promote dissolution of P from BC (Leinweber et al., 2019; Zimmer et al., 2018; Zimmer et al., 2019). The BC fertilization increased plant P uptake compared to no-fertilization (Little et al., 2017; Zwetsloot et al., 2016). Results of these studies suggest that crops such as wheat and grass, with relatively long growth periods and developed root systems, could have a higher agronomic efficiency than fast growing vegetables when considering slowly released P from BC-based fertilizers (Leinweber et al., 2019). Moreover, the surface of BC can be enriched with up to 20% (w/w) elemental sulfur (S) (BC^{plus} patent DE102011010525). This occurs through the adsorption of gaseous sulfur from biogas streams, and could increase the solubility of BC P in the soil (Zimmer et al., 2018). A so-called "in situ digestion" process may be involved which promotes apatite dissolution through the release of H_2SO_4 from microbial sulfoxidation (Fan et al., 2012). Previous batch and pot experiments have confirmed a higher solubility of BC^{plus} compared to BC (Morshedizad et al., 2018; Zimmer et al., 2019). This implies that BC^{plus}, which is recycled slaughterhouse waste and biogas streams, could be a suitable alternative to RP fertilizers (Zimmer et al., 2018).

However, to be useful for organisms and plants, the released P from fertilizer must be both bioavailable (present in a suitable chemical form) and bioaccessible (physically accessible). The bioaccessibility of P is largely controlled by soil aggregates, with the incorporation and release of P during aggregate formation and breakdown playing a vital role in nutrient storage and cycling (Bronick and Lal, 2005; Six et al., 2004). Over the past several decades, extensive works has been done investigating and comparing the effects of P fertilization on P speciation and availability in soils (Ajiboye et al., 2008; Alamgir and Marschner, 2013; Baggie et al., 2004; Koch et al., 2018; Siebers et al., 2021; Vogel et al., 2017). However, little is known about the fate of fertilizer P within soil aggregates, or the effects of P fertilization on various P pools within soil aggregates (Garland et al., 2018; Wan et al., 2020). Additionally, no information is available about the fate of fertilizer P from either BC or BC^{plus}. Soil aggregates consist of macro, micro, and nanoscale aggregates composed of inorganic (minerals) and organic (organic matter, microbial biomass/debris) materials resulting from various physical, chemical, and biological processes (Totsche et al., 2018). Soil microaggregates (< 250 µm) possess a relatively high stability and persistence and are strongly linked with the major biological processes controlling the turnover of nutrients. In the literature, it has been shown that there is a faster potential P turnover rate in large microaggregates than in small microaggregates (Siebers et al., 2018). Knowledge of the functional relationship between soil aggregates and P is key to evaluating the potential of soils to store and supply fertilizer P to plants. Improving our understanding of the fate of fertilizer P and its transformation and cycling within the soil aggregates is important for the development of sustainable fertilizer management.

We hypothesize that P introduced through BC and BC^{plus}, due to their differences in pH and solubility (Grafe et al., 2021; Morshedizad et al., 2018; Zimmer et al., 2018), may perform differently from each other, as well as from highly water soluble triple superphosphate (TSP) fertilizer, in soil aggregates and thus affecting soil P availability and forms. The objective of this study was to determine for the first time the fate of fertilizer P from BC, BC^{plus}, and TSP in different soil aggregate size fractions under field conditions. Samples were taken from a five-year (one crop rotation) experiment site, which was the first BC-based field fertilization trial. We applied Hedley sequential P extraction for soil aggregates and different P forms and availabilities (labile, moderately labile, and stable P) were evaluated. This study provides essential knowledge on the availability, transformation, and storage of P within different soil aggregate size fractions after continuous BC and BC^{plus} fertilizations, giving insight into the optimum application of these promising fertilizer resources.

2. Materials and methods

2.1. Study site and experimental design

The study site is arable land located near Braunschweig, Germany (10° 27´ E; 52° 18´ N, elevation 81 m a.s.l.) with a mean annual temperature of 9 °C and a mean annual precipitation of 620 mm. The soil at the site is described as Haplic Luvisol and Dystric Cambisol (IUSS Working Group WRB, 2015) and is built from sandy fluvial sediments overlaid with sandy loess. This site was subject to continuous long-term P fertilization from 1985 to 2008, followed by extensive management as grassland from 2009 to 2012, and then converted to arable land for the preparation of the current study. The application of different dosages of P fertilizer P to randomly designed plots from 1985-2008 (for more details see Vogeler et al. (2009)) left randomly distributed plots with different concentrations of calcium acetate lactate extractable P (P-CAL). These were assigned to initial soil P-test classes (iSPTC) based on their topsoil P-CAL concentrations, i.e., iSPTC-A (severely deficient, < 15 mg P-CAL kg^{-1}), iSPTC-B (deficient, 15 to 30 mg P-CAL kg^{-1}), and iSPTC-C (sufficient, 31 to 60 mg P-CAL kg^{-1}), respectively (Wiesler et al., 2018). Only iSPTC-A and iSPTC-C plots were involved in the present study. Measurements of initial soil characteristics for iSPTC-A and iSPTC-C bulk soils revealed levels of total carbon C: 13 and 14 g kg^{-1}, total nitrogen (N): 10 and 10 g kg^{-1}, total P: 349 and 520 mg kg^{-1}, and pH: 5.1 and 5.2, respectively. For more details on former field characteristics and site management see Panten and Leinweber (2020).

The present study began in the autumn of 2013 with four different P fertilization treatments on iSPTC-A and iSPTC-C bulk soils: 1) control, without P addition, described as No-P; 2) triple superphosphate, TSP; 3) bone char, BC; and 4) bone char enriched with elemental sulfur, BC^{plus}. Each treatment had three replicated plots (5.75 m × 17.5 m), which were arranged in a completely randomized block design. All P treatments (TSP, BC, and BC^{plus}) received 45 kg P ha^{-1} $year^{-1}$. The plots received a combination of chisel ploughing and conventional ploughing to a depth of 25 cm before yearly sowing (5-year crop rotation: winter barley, winter oilseed rape, winter wheat, lupin, and winter rye). For details regarding fertilizations with other elements as well as crop yields and P uptake of plants in response to the P treatments refer to Panten and Leinweber (2020).

The BC was manufactured by pyrolysis of rendered (de-fatted) crushed bovine bones at around 800 °C. Subsamples of BC were surface-modified by adsorbing H_2S (BC^{plus}) from a biogas stream according to the procedure described in patent DE102011010525. The total P contents of the applied P fertilizers are 148 g kg^{-1} (BC), 107 g kg^{-1} (BC^{plus}), and 200 g kg^{-1} (TSP). Properties of both BC-based fertilizers have been previously reported (Zimmer et al., 2018).

2.2. Soil sampling and soil aggregates separation

In the present study, we investigated soil samples before the start of the trial (August 21, 2013) and after completion of the first 5-year crop rotation (July 20, 2018). For soil sampling, eight soil cores were taken per treatment to a depth of 30 cm, and then combined into a composite bulk sample. The samples were air-dried and sieved through 2 mm (as bulk soil) and stored in plastic bags before soil aggregate separation and further analyses.

The bulk soil was separated into four soil size fractions slightly adjusted from size range defined by Totsche et al. (2018), namely (i) small macroaggregates (SMaA, 250 to 2000 μm); (ii) large microaggregates (LMiA, 53 to 250 μm); (iii) small microaggregates (SMiA, 1 to 53 μm), and (iv) composite building units (BU, < 1 μm). For size fractionation, a combination of wet sieving, centrifugation, and tangential flow filtration (TFF) was applied (Dalwadi and Sunderland, 2007; Six et al., 2000; Tang et al., 2009). Bulk soil (< 2 mm) was firstly immersed in deionized water on top of the two-sieves stack (mesh size 250 and 53 μm) and manually shaken up and down. The fractions remaining on the 250 μm and 53 μm sieves were designated as SMaA and LMiA, respectively. The wet-sieving procedure took 1 hour for 40.0 g of soil samples using 10 cm diameter sieves. The 1 to 53 µm aggregates were separated by centrifugation at 4000 rcf for 2 min calculated using Stork's law (Henderson et al., 2012) and the solids were transferred to a beaker for drying (as SMiA). The supernatant was passed through a TFF system (Minmate™ TFF Capsule (1 KDa m-polyethersulfone membrane, PALL Life Sciences, USA) associated with pressure gauges and a peristaltic pump (Cole-Parmer, Masterflex L/S)). The concentrated supernatant was collected and dried (as BU). All four soil size fractions were oven dried at 40 °C, weighed, and stored for further analyses.

2.3. Soil analyses

The mass distribution proportion of soil aggregates was calculated by dividing the weight of each aggregate size fraction by the weight of bulk soil used in the wet sieving procedure. The mean weight diameter (MWD, µm), an evaluation parameter for changes in soil aggregate stability, was calculated according to the following equation:

$$\text{MWD} = \sum_{x=1}^{n} w_x \times \bar{d}_x \qquad \text{(Eq. 1)}$$

where n is the number of aggregate size fractions, w_x is the ratio of the weight of the x^{th} fraction to the weight of bulk soil used in the wet sieving, and $\bar{d}_x$ is the mean diameter of the x^{th} fraction (µm). Total elemental contents of Ca, Mg, and iron (Fe) were determined after microwave-assisted digestion of 150 mg soil samples with 0.7 mL HNO_3 and 2 mL HCl using inductively coupled plasma-optical emission spectroscopy (ICP-OES; Thermo Fisher iCAPTM 7600). The contents of total C, N, and S were analyzed by dry combustion followed by heat conductivity detection of the released trace gases (vario MICRO cube, Elementar, Hanau, Germany).

2.4. Sequential P fractionation

For the sequential P fractionation of soil aggregates, a slightly modified Hedley sequential P extraction procedure was applied (Hedley et al., 1982; Negassa et al., 2010; Schmitt et al., 2017). Individual samples of 0.5 g (0.2 g for BU) were weighed into 50 mL (15 mL for BU) centrifuge tubes and sequentially extracted with 30 mL (12 mL for BU) of: (1) ultrapure deionized water, (2) 0.5 M $NaHCO_3$, (3) 0.1 M NaOH, and (4) 1 M H_2SO_4. Each suspension was shaken at 250 rpm for 18 h followed by centrifugation at 5000 rcf for 20 min. The sequentially extracted P was referred to different P pools hereafter. The concentration of total P (P_t) in each extract was determined by ICP-OES. Inorganic P (P_i) concentration in each extract was measured with the molybdate blue colorimetric method using a UV-Vis spectrometer at a wavelength of 890 nm (Nagul et al., 2015). Organic P (P_o) concentrations in the H_2O, $NaHCO_3$, and NaOH extracts were calculated as the differences between the P_t and P_i of each of these three P pools. The extracted P pools were further designated as follows: (1) H_2O-P + $NaHCO_3$-P = labile P, (2) NaOH-P = moderately labile P, and (3) H_2SO_4-P = stable P. The sum of these three P pools (labile, moderately labile and stable P) is referred to as total P and the proportion of each P pool to the total extracted P was calculated for every size fraction. In addition, the P mass proportion of each size fraction to the sum of P of all four soil size fractions was calculated as follows:

$$\text{P proportion of } x^{th} \text{ fraction (\%)} = 100 \times \frac{P_x \times m_x}{\sum_{x=1}^{n} P_x \times m_x} \qquad \text{(Eq. 2)}$$

where n is the number of aggregate size fractions, P_x is the P content (g kg^{-1} fraction) of x^{th} fraction, and m_x is the mass (g) of x^{th} fraction.

2.5. Statistical analyses

Data analyses and graph plotting were performed with RStudio software version 3.6.3 (R Core Team, 2021). Normality and homogeneity of variance assumptions of data sets were tested by Shapiro-Wilk and Levene's test, respectively (Alboukadel, 2021). If the assumptions were verified, a two-way mixed ANOVA was performed to compare means of all treatments (independent factor) and aggregate size fractions (dependent factor) for each soil P class (i.e., iSPTC-A and -C) separately. The assumption of sphericity was tested using the Mauchly's tests, and, if the assumption was violated the Greenhouse-Geisser sphericity correction was applied (Alboukadel, 2021). If the assumptions (normality and homogeneity of variances) of the two-way mixed ANOVA were violated, the non-parametric Friedman's ANOVA was used (Field et al., 2012). Significant two-way interactions of the two parameters – treatments and aggregate size fractions – were also tested, but none were found. Therefore, we performed multiple paired t-tests for the treatment ignoring size fraction, and vice versa. The *p* values were adjusted using the Bonferroni multiple testing correction method. Paired *t*-tests were also applied to compare means of each sample collected in 2013 and 2018, for each treatment, and in each aggregate size fraction (Alboukadel, 2021; Field et al., 2012). The statistical significance was accepted when $p < 0.05$.

3. Results

3.1. Mass distribution and MWD of soil size fractions

Aggregate mass proportions declined in the order of SMiA > LMiA ≈ SMaA > BU and were consistent across treatments in both soil P classes (iSPTC-A and -C) (**Figure 1**). The mass proportions of SMiA ranged from 32.5±0.1 (mean±sd) to 46.5±1.3%, LMiA from 25.1±0.4 to 33.0±0.3%, SMaA from 23.5±0.1 to 35.4±0.4%, and BU from 0.4±0.2 to 1.9±0.0%. When comparing the aggregate mass proportions between 2013 and 2018, most treatments (No-P, TSP, and BC) had insignificant effects althrough the BC^{plus} treatment significantly decreased the mass proportion of LMiA from 31.0 (2013) to 27.4% (2018) in iSPTC-A soil. After five years of field applications, only the mass proportion of LMiA in iSPTC-A soil showed significant increases for all P fertilization treatments (TSP 26.4%, BC 26.7%, BC^{plus} 27.4%) when compared to the No-P treatment (25.9%). In addition, the TSP treatment (0.90%) significantly decreased the mass proportion of BU in iSPTC-A soil compared to the BC^{plus} treatment (1.02%), while No-P and BC treatments had insignificant effects on BU mass proportion. The MWD of all treatments ranged between 317 to 449 µm (**Figure S1**; Supplementary Data). In the No-P treatment for iSPTC-C soil, the MWD had a significant 8% decrease from 2013 (381 µm) to 2018 (352 µm) . Similarly, the MWDs of TSP, BC, and BC^{plus} treatments decreased by 8.7%, 2.4%, 8.4% for iSPTC-A soil, and 3.1%, 5.6%, 13.0% for iSPTC-C soil after five years, respectively.

3.2. Total elemental contents and P proportions in soil size fractions

The total contents of C, N, S, P, Ca, Fe, and Mg increased with decreasing soil size fractions, irrespective of fertilization treatment and soil initial P classes (**Table S1** and **S2**; Supplementary Data). Generally, all total elemental contents in the BU were significantly higher (2 to 9 times) than that in SMaA, LMiA, and SMiA, while there were similar, although insignificant elemental concentrations among the latter three soil size fractions. In each soil size fraction, elemental contents were generally not significantly affected by different P fertilizer treatments. In line with expectations, the Ca contents and bulk soil pH values increased in all treatments and soil P classes after five years.

The proportion of each soil size fraction P mass to the sum of P mass of all soil size fractions was calculated using Eq. 2. For both soil P classes, all treatments showed the fraction containing the largest mass proportion of total P to be SMiA (37 to 62%) followed by LMiA (16 to 34%), SMaA (13 to 29%), and BU (3.5 to 8.2%) (**Figure 2**). The P mass proportions of most soil size fractions were not affected by the different fertilizer treatments; however, in the iSPTC-A soil, TSP application significantly increased the mass proportion of P in the LMiA (33%) compared to that of No-P (28%) and BC (26%) treatments. Furthermore, P mass proportions in the LMiA in the iSPTC-C soil increased significantly (from 21% to 28%) after five years of No-P fertilization.

3.3. Sequentially extracted P pools in soil size fractions

When evaluating the P concentration in relation to the mass of each size fraction (mg P kg^{-1} size fraction) for extracted different P pools, the P concentrations of each soil size fraction increased in the order of H_2O-P_i < H_2O-P_o < $NaHCO_3$-P_o ≈ $NaHCO_3$-P_i < NaOH-P_i ≈ H_2SO_4-P < NaOH-P_o irrespective of the treatment or iSPTC soil type (**Table S3** and **S4**; Supplementary Data). Within given treatment the concentrations of most P pools increased with decreasing aggregate size. Only the H_2O-extractable P pool (H_2O-P_i and H_2O-P_o) showed no clear trend.

Most of the extracted P pools did not change significantly after 5-years of BC and BC^{plus} fertilizations in either iSPTC soil type. The highly soluble TSP was the only treatment that showed a significant increase in concentration in most P pools, with the exceptions being NaOH-P_o and H_2SO_4-P in iSPTC-A soil. This was especially apparent in the smaller size fractions (SMiA and BU) (**Table S3**; Supplementary Data). For iSPTC-C soil, such systematic changes in P concentrations were not observed, although ; concentrations of NaOH-P_o and H_2SO_4-P did significantly increase over time in BU under TSP treatment (**Table S4**; Supplementary Data). In soils supplemented with BC, the concentrations of $NaHCO_3$-P_i in SMaA and SMiA decreased after five years: -30% and -18%, respectively. An even more pronounced decrease was observed for iSPTC-C soil with No-P after 5 years: -28% of H_2O-P_i in SMaA, -54% of H_2O-P_o in BU, -33% and -22% of $NaHCO_3$-P_i in SMaA and LMiA, and -9% of NaOH-P_i in BU.

Overall, the TSP, BC, and BC^{plus} treatments increased the total extractable P_i (sum of H_2O-P_i, $NaHCO_3$-P_i, NaOH-P_i, and H_2SO_4-P) from 714 to 853 mg kg^{-1} in BU; in the TSP, from 192 to 235 mg kg^{-1} in SMiA, and 176 to 214 mg kg^{-1} in LMiA for iSPTC-A soil **(Table S3**; Supplementary Data). A similar increasing trend of total extractable P_i was not detected for iSPTC-C soil.

3.4. Labile, moderately labile, and stable P pools in soil size fractions

The sequentially extracted P pools can be further assigned into three P pools differing in plant availability, i.e., labile P (sum of H_2O-P_i, H_2O-P_o, $NaHCO_3$-P_i, and $NaHCO_3$-P_o), moderately labile P (sum of NaOH-P_i and NaOH-P_o), and stable P (H_2SO_4-P) pools. When relating the P mass of each P pool and size fraction to the total mass of the bulk soil (mg P kg^{-1} soil), the concentrations of the three P pools followed the order of labile P < stable P < moderately labile P and increased with decreasing soil size fraction. An exception to this was BU which exhibited the lowest concentrations for each of the three P pools in all treatments and iSPTC soil types (**Figure 3)**. The highest concentrations of all three P pools were found in SMiA, irrespective of treatment and iSPTC soil type. Within a treatment, the labile P concentration in SMiA was generally significantly higher than that found in other soil size fractions, with the exceptions of TSP and BC^{plus} treatments in iSPTC-A soil. Moderately labile P was not significantly different between SMaA and LMiA irrespective of treatment, except for TSP in iSPTC-A soil. There were no general trends observed for stable P. In most cases, there were no significant differences of P pool concentrations between various treatments. Significant variations were only apparent for higher concentrations of labile P in LMiA under TSP compared to BC treatment in iSPTC-C soil (**Figure 3**).

4. Discussion

4.1. Size distribution and elemental compositions of soil aggregates

Before the trial was established in 2013, the field site had been managed as grassland for four years (from April 2009 to April 2013). From 2013 to 2018, the time frame of this study, the site was ploughed annually. Such conversion into cropland results in the breakdown of macroaggregates (Spohn and Giani, 2011). Since macroaggregates are weak associations of biodegradable compounds and microaggregates (Tisdall and Oades, 1982), they easily disintegrate under ploughing (Paul et al., 2013), leading to release of microaggregates. In this study, the mass proportion of soil size fractions decreased in the order of SMiA > LMiA ≥ SMaA ≫ BU, irrespective of treatment (**Figure 1**), which is in line with results described in the literature (Fernández-Ugalde et al., 2013; Garland et al., 2018; Krause et al., 2018; Zhang et al., 2020).

This release of microaggregates may be partially responsible for the significant increase seen in the LMiA mass proportion after five years of P fertilization compared to No-P. Fertilization with P is also likely stimulated plant and/or microbe growth, leading to an increase in organic binding agents such as polysaccharides, roots, microbial hyphae or debris, which could have enhanced soil microaggregation (Tisdall and Oades, 1982). The concomitant decrease of the BU mass in iSPTC-A soil after the addition of highly plant available TSP could therefore be a result of incorporation of BU into newly formed microaggregates (Jastrow, 1996; Tisdall and Oades, 1982). Furthermore, all three P fertilizers contained significant amounts of Ca^{2+}, which can potentially enable bonding between clay and organic matter as clay-polyvalent metal-organic matter complexes, which play a critical role in microaggregate formation (Tisdall and Oades, 1982). While the P fertilization contributed an additional annual Ca input of 21 kg ha^{-1} for BC and BC^{plus}, and ~ 60 kg ha^{-1} for TSP, this is negligible when considering the amount of Ca applied to all treatments by liming twice during the experimental duration (909 + 1441 kg Ca ha^{-1}). This also explains the significant increase of both Ca concentration and soil pH from 2013 to 2018 (**Table S1** and **S2**; Supplementary Data) (Haynes and Naidu, 1998). This would suggest that the significant increase of LMiA mass proportion in all P fertilized treatments compared to No-P (at iSPTC-A soil) is unlikely to be explained by Ca^{2+} enhanced microaggregate formation as No-P also received twice liming. Therefore, it seems that even under the conditions of grass to crop land use conversion, fertilization with TSP or BC-based materials could enhance soil micro-aggregation at P deficient soils.

As shown in **Table S1** and **S2** (Supplementary Data), total elemental concentrations increased with decreasing aggregate size, which is in agreement with previously reported results (Fernández-Ugalde et al., 2013; Luo et al., 2011; Wright, 2009; Zhang et al., 2003). This can be explained by the accumulation of soil organic matter and other elements into small size fractions due to an increase in the specific surface area and a reduced presence of primary mineral particles like sand and silt (Garland et al., 2018; Kahle et al., 2002; Kennedy et al., 2002). In our study, the highest elemental concentrations were found in BU, while the absolute mass of BU was the lowest (0.4 to 1.9%) of all size fractions. Although the contribution to total plant P uptake of P bound in BU is likely to be low, it is not known whether BU play a role in providing P in the micro- or nanoscale (Sinaj et al., 1997). Santner et al. (2012) showed that nanoparticle bound P can buffer the P concentration if plant uptake of P is limited by diffusion of free P to the plant roots. BU could also facilitate the movement/transport of soil P as BU is easily transported via soil water flows (Gu et al., 2020; Siebers et al., 2023). Moreover, plant roots may be able to internalize BU either directly or after partial dissolution with the help of root exudates using mechanisms have been reported for engineered nanoparticles (Jia et al., 2022; Wagener et al., 2019). The contribution of BU to total plant P uptake would be an interesting avenue for further research.

As reported by Wang et al. (2001), plant uptake of P increased with increasing aggregate size. This can be attributed to a decrease in aggregate stability, reduced P fixation, and an associated increase in P release from large aggregates. The observed significant increase of P proportion after TSP addition and of P concentration after BC^{plus} addition in LMiA in iSPTC-A soil (**Figure 2** and **Table S1**; Supplementary Data) indicated that fertilizer P in excess of that needed by crops accumulated in this size fraction. These results suggest that modification with elemental sulfur in BC^{plus} not only increases its solubility, potentially providing more plant available P than untreated BC, but also results in the accumulation of excess fertilizer P in a bioaccessible form similar to TSP. Meanwhile, SMiA, with the highest mass proportion, contained the largest P proportions even though its P concentration was only accounted for ~ 30% to that of BU. As SMiA had the highest P mass proportion and BU had the highest P concentration, in addition to both particle sizes being < 53 μm, they would contribute to soil P loss especially under erosion events (Siebers et al., 2023). Hence, for agricultural managements and control of non-point source pollution, more attention should be paid to these two size fractions.

4.2. Variations of P pools in soil size fractions

The order of increasing P concentration in the individual P pools (i.e., H_2O-P_i ≈ H_2O-P_o < $NaHCO_3$-P_o < $NaHCO_3$-P_i < NaOH-P_i ≈ H_2SO_4-P < NaOH-P_o, **Table S3** and **S4**; Supplementary Data) was in line with the literature, including the expectation that labile P pools had lower concentrations than stable P pools (Ranatunga et al., 2013; Siebers et al., 2021). Although H_2O-P_i and H_2O-P_o did not follow the general trend of increasing P concentrations with decreasing size, this may be due to methodological artifacts of the wet sieving method we used to fractionate the soil aggregates. During aggregates separation, ultrapure deionized water (about 600 mL) was used, which could result in the loss of a proportion of the H_2O-P pool before sequential extraction. When estimating the amount of P that had been lost during wet-sieving, the lost P approximately accounted for 1.6 to 29.5% of H_2O-P (see more details in the Supplementary data). Hence, the effect of wet-sieving to H_2O-P should not be neglected. Other factors may also contribute to similar concentrations of H_2O-P among four the soil size fractions. Before extraction, the soil size fractions were oven-dried at 40 ℃ to constant weight. As Wang et al. (2020) reported, an air-drying step increased the Hedley extracted labile P pool due to its influence on microbial biomass P and soil organic matter. The oven-drying step we applied here may bring about changes in soil H_2O-P and other labile P pools as well. More studies are needed to elucidate the effects of various drying processes on Hedley extracted P pools.

After five years of P fertilization, most pronounced treatment effects were visible for the TSP treatment, which significantly increased all P pools in iSPTC-A soil, apart from the NaOH-P_o and H_2SO_4-P pools in most size fractions (**Table S3**; Supplementary Data). This could be a result of the higher stability of P extracted in these P pools. The NaOH-P represents moderately labile inorganic and organic P that are most likely sorbed and/or fixed by aluminum- and iron (hydr)oxides (accessory minerals) and P in soil organic matter being only potentially bioavailable (Cross and Schlesinger, 1995; Tisdall and Oades, 1982). The H_2SO_4-P represents mostly insoluble (stable) P associated mainly with Ca and Mg minerals and is in occluded or non-occluded forms (Hou et al., 2018). Therefore, the turnover times of these two P pools are long and the five-year durations of this study might not be sufficient to show effects even after application of a highly soluble P fertilizer like TSP. This same situation was also reported by Siebers et al. (2021) who studied P pools in four long-term trials. Interestingly, the SMiA H_2SO_4-P proportions did significantly increase after five years of BC application. However, this effect is not likely to be a result of P dissolution from BC and subsequent fixation of released P in moderately labile and stable P pools, but rather a sequestration of decomposed BC particles in the SMiA size range.

The observed significant reduction of $NaHCO_3$-P_o concentrations (**Table S3**; Supplementary Data) in SMaA and BU in the No-P treatment of iSPTC-A soil might be a result of an adaption of the microbial community to lower P concentrations leading to higher mineralization rates of $NaHCO_3$-P_o (Grafe et al., 2021). Furthermore, liming and the associated increase in soil pH may have affected phosphatase activities, further promoting $NaHCO_3$-P_o mineralization (Acosta-Martinez and Tabatabai, 2000). The $NaHCO_3$-P_o represents labile, mineralizable P_o (Hou et al., 2018), which is less stable and more susceptible to microbial mineralization than NaOH-P_o under P limitation (No-P treatment) (Ranatunga et al., 2013). The significant increase of $NaHCO_3$-P_o in the TSP treatment was in line with the idea that the mineralization of P_o is controlled by the supply and demand of P (McGill and Cole, 1981). The observed significant increase of $NaHCO_3$-P_i in BU in the TSP treatment of iSPTC-A soil compared to the No-P treatment (**Table S3**; Supplementary Data) was probably a result of the high specific surface area of the large number of adsorption sites of BU relative to the larger size factions (Wang et al., 2001).

Our findings suggested that five years of field fertilization with both highly soluble TSP and slow-release BC and BC^{plus} did not significantly affect the moderately labile and stable P pools, while TSP contributed significantly to the labile P pool accrual. This enrichment of soil labile P could lead to a high risk of P loss and the resulting ecological problems due to particle facilitated P leaching or runoff, while results in the same trial gave no indication on this (Kruse et al., 2022). Under P limitation, the moderately labile organic P pool in the loosely aggregated size fraction (SMaA) and the smallest size fraction (BU), which have the highest P contents are more prone to be mineralized and to replenish soil available P, although this needs further investigation. As reported by Panten and Leinweber (2020), the mean yields during one crop rotation of the present trial showed insignificant differences among treatments, with only insignificant variation of crop yields in the order of BC < BC^{plus} < TSP under P limitation. Thus, we recommend that for P sufficient soils, BC materials have the potential as substitute for TSP (especially in acidic soils), which will neutralize soil pH and sustain plant labile P in a slow-release and eco-friendly way. For P deficient soils, BC and especially BC^{plus} may be applied in combination with TSP, in which way TSP could supply P quickly while BC materials could serve as a slow-release fertilizer. However, this combination should be tested with longer trial duration and more soil types before it could be recommended to farmers.

5. Conclusions

Previous lab and pot experiments have indicated that BC, and in particular BC^{plus}, may be promising recycled material alternatives for conventional mineral based P fertilizers such as TSP. The fate of fertilizer P in the soil, and thus its agronomic value, is largely controlled by soil aggregates. This is because the incorporation and release of P during aggregate formation and breakdown plays a vital role in bioaccessibility, storage, and cycling of soil P. This study is the first to compare the five years of repeated field P fertilization with TSP, BC, and BC^{plus} on the fate of fertilizer P into soil P pools within different aggregate size fractions. After five years (one crop rotation), the treatment effects were mostly insignificant for concentrations and proportions of P pools. The reported higher solubility of TSP compared to BC was reflected in the significantly higher concentrations of labile P in TSP compared to those in the BC treatments in LMiA of iSPTC-C soil as well as in SMiA and BU of iSPTC-A soil. The fact that the differences between TSP and BC^{plus} were not significant indicates sulfur modification of BC can improve P availability of BC at the field scale. As TSP is highly soluble and quick in P supply, TSP released labile P would be fixed by soil aggregates and may lost under rainfall events. For soils sufficient in P, BC and especially BC^{plus} could be alternatives for TSP to maintain concentrations in labile soil P pools and decrease particle facilitated P losses. Indeed, longer-term field trials with more soil types are needed to fully elucidate the fertilization effects of BC materials on various P pools in soil size fractions.

Appendix A. Supplementary data

Acknowledgements

Yunsheng Jia is grateful to the Chinese Scholarship Council (CSC201808320415) for supporting his study in Germany. This project was funded in the frame of the Bioeconomy 2030 initiative of the Federal Ministry for Education and Research (BMBF; call: BonaRes; project InnoSoilPhos: No 031A558G, 031B0509E, and 031B0509D). We acknowledge the support of Peter Narf for collecting field soil samples, Dr. Volker Nischwitz (ZEA 3, FZ Jülich) for ICP-MS measurements, and Ursula Paffen (IBG 3, FZ Jülich) for assistance with UV-VIS spectrometer measurements.

References

Acosta-Martinez, V., Tabatabai, M.A., 2000. Enzyme activities in a limed agricultural soil. Biol. Fertil. Soils 31, 85-91. https://doi.org/10.1007/s003740050628.

Ajiboye, B., Akinremi, O.O., Hu, Y.F., Jürgensen, A., 2008. XANES speciation of phosphorus in organically amended and fertilized vertisol and mollisol. Soil Sci. Soc. Am. J. 72(5), 1256-1262. https://doi.org/10.2136/sssaj2007.0078.

Alamgir, M., Marschner, P., 2013. Short-term effects of application of different rates of inorganic P and residue P on soil P pools and wheat growth. J. Soil Sci. Plant Nutr. 176(5), 696-702. https://doi.org/10.1002/jpln.201200290.

Alboukadel, K., 2021. rstatix: Pipe-friendly framework for basic statistical tests, Online.

Baggie, I., Rowell, D.L., Warren, G.P., Robinson, J.S., 2004. Utilisation by upland rice of plant residue- and fertiliser-phosphorus in two tropical acid soils. Nutr. Cycling Agroecosyst. 69(1), 73-84. https://doi.org/10.1023/b:fres.0000025292.05519.46.

Bronick, C.J., Lal, R., 2005. Soil structure and management: A review. Geoderma 124(1-2), 3-22. https://doi.org/10.1016/j.geoderma.2004.03.005.

Cordell, D., Drangert, J., White, S., 2009. The story of phosphorus: Global food security and food for thought. Glob. Environ. Change 19(2), 292-305. https://doi.org/10.1016/j.gloenvcha.2008.10.009.

Cross, A.F., Schlesinger, W.H., 1995. A literature review and evaluation of the Hedley fractionation: Applications to the biogeochemical cycle of soil phosphorus in natural ecosystems. Geoderma 64, 197-214. https://doi.org/10.1016/0016-7061(94)00023-4.

Dalwadi, G., Sunderland, V.B., 2007. Purification of PEGylated nanoparticles using tangential flow filtration (TFF). Drug Dev. Ind. Pharm. 33(9), 1030-1039. https://doi.org/10.1080/03639040601180143.

Desmidt, E., Ghyselbrecht, K., Zhang, Y., Pinoy, L., Van der Bruggen, B., Verstraete, W., Rabaey, K., Meesschaert, B., 2015. Global phosphorus scarcity and full-scale P-recovery techniques: A review. Crit. Rev. Environ. Sci. Technol. 45(4), 336-384. https://doi.org/10.1080/10643389.2013.866531.

Fan, X.H., Schnug, E., Haneklaus, S., Li, Y.C., 2012. In situ digestion of rock phosphates to mobilize plant-available phosphate for organic farming. Commun. Soil Sci. Plant Anal. 43(17), 2191-2201. https://doi.org/10.1080/00103624.2012.708073.

Fernández-Ugalde, O., Barré, P., Hubert, F., Virto, I., Girardin, C., Ferrage, E., Caner, L., Chenu, C., 2013. Clay mineralogy differs qualitatively in aggregate-size classes: Clay-mineral-based evidence for aggregate hierarchy in temperate soils. Eur. J. Soil Sci. 64(4), 410-422. https://doi.org/10.1111/ejss.12046.

Field, A., Miles, J., Field, Z., 2012. Discovering statistics using R. SAGE Publications Ltd.

Garland, G., Bünemann, E.K., Oberson, A., Frossard, E., Snapp, S., Chikowo, R., Six, J., 2018. Phosphorus cycling within soil aggregate fractions of a highly weathered tropical soil: A conceptual model. Soil Biol. Biochem. 116, 91-98. https://doi.org/10.1016/j.soilbio.2017.10.007.

Glaesner, N., Hansen, H.C.B., Hu, Y.F., Bekiaris, G., Bruun, S., 2019. Low crystalline apatite in bone char produced at low temperature ameliorates phosphorus-deficient soils. Chemosphere 223, 723-730. https://doi.org/10.1016/j.chemosphere.2019.02.048.

Grafe, M., Kurth, J.K., Panten, K., Raj, A.D., Baum, C., Zimmer, D., Leinweber, P., Schloter, M., Schulz, S., 2021. Effects of different innovative bone char based P fertilizers on microbiota catalyzing P turnover in agricultural soils. Agr. Ecosyst. Environ. https://doi.org/10.1016/j.agee.2021.107419.

Gu, S., Gruau, G., Dupas, R., Jeanneau, L., 2020. Evidence of colloids as important phosphorus carriers in natural soil and stream waters in an agricultural catchment. J. Environ. Qual. 49(4), 921-932. https://doi.org/10.1002/jeq2.20090.

Haynes, R.J., Naidu, R., 1998. Influence of lime, fertilizer and manure applications on soil organic matter content and soil physical conditions: A review. Nutr. Cycl. Agroecosyst. 51(2), 123-137. https://doi.org/10.1023/A:1009738307837.

Hedley, M.J., Stewart, J.W.B., Chauhan, B.S., 1982. Changes in inorganic and organic soil phosphorus fractions induced by cultivation practices and by laboratory incubations. Soil Sci. Soc. Am. J. 46(5), 970-976. https://doi.org/10.2136/sssaj1982.03615995004600050017x.

Henderson, R., Kabengi, N., Mantripragada, N., Cabrera, M., Hassan, S., Thompson, A., 2012. Anoxia-induced release of colloid- and nanoparticle-bound phosphorus in grassland soils. Environ. Sci. Technol. 46(21), 11727-11734. https://doi.org/10.1021/es302395r.

Holford, I.C.R., 1997. Soil phosphorus: Its measurement, and its uptake by plants. Aust. J. Soil Res. 35(2), 227-240. https://doi.org/10.1071/S96047.

Hou, E.Q., Tan, X., Heenan, M., Wen, D.Z., 2018. A global dataset of plant available and unavailable phosphorus in natural soils derived by Hedley method. Sci. Data 5, 13. https://doi.org/10.1038/sdata.2018.166.

IUSS Working Group WRB, 2015. World Reference Base for Soil Resources 2014, FAO, Rome, Italy.

Jastrow, J.D., 1996. Soil aggregate formation and the accrual of particulate and mineral associated organic matter. Soil Biol. Biochem. 28(4-5), 665-676. https://doi.org/10.1016/0038-0717(95)00159-X.

Jia, Y.S., Klumpp, E., Bol, R., Amelung, W., 2022. Uptake of metallic nanoparticles containing essential (Cu, Zn and Fe) and non-essential (Ag, Ce and Ti) elements by crops: A meta-analysis. Crit. Rev. Environ. Sci. Technol., 1-22. https://doi.org/10.1080/10643389.2022.2156225.

Kahle, M., Kleber, M., Jahn, R., 2002. Carbon storage in loess derived surface soils from central Germany influence of mineral phase variables. J. Plant Nutr. Soil Sci. 165(2), 141-149. https://doi.org/10.1002/1522-2624(200204)165:2<141::AID-JPLN141>3.0.CO;2-X.

Kennedy, M.J., Pevear, D.R., Hill, R.J., 2002. Mineral surface control of organic carbon in black shale. Science 295(5555), 657-660. https://doi.org/10.1126/science.1066611.

Koch, M., Kruse, J., Eichler-Löbermann, B., Zimmer, D., Willbold, S., Leinweber, P., Siebers, N., 2018. Phosphorus stocks and speciation in soil profiles of a long term fertilizer experiment: Evidence from sequential fractionation P K edge XANES and 31P NMR spectroscopy. Geoderma 316, 115-126. https://doi.org/10.1016/j.geoderma.2017.12.003.

Krause, L., Rodionov, A., Schweizer, S.A., Siebers, N., Lehndorff, E., Klumpp, E., Amelung, W., 2018. Microaggregates stability and storage of organic carbon is affected by clay content in arable Luvisols. Soil Tillage Res. 182, 123-129. https://doi.org/10.1016/j.still.2018.05.003.

Kruse, J., Panten, K., Siebers, N., 2022. The fate of phosphorus from bone char-based fertilizers in soil pools in a 5-year crop rotation. Nutr. Cycling Agroecosyst. 124(2), 263-277. https://doi.org/10.1007/s10705-022-10228-y.

Leinweber, P., Hagemann, P., Kebelmann, L., Kebelmann, K., Morshedizad, M., 2019. Bone char as a novel phosphorus fertilizer, Phosphorus Recovery and Recycling, pp. 419-432.

Little, N.G., Mohler, C.L., Ketterings, Q.M., DiTommaso, A., 2017. Effects of organic nutrient amendments on weed and crop growth. Weed Sci. 63(3), 710-722. https://doi.org/10.1614/ws-d-14-00151.1.

Luo, X.S., Yu, S., Li, X.D., 2011. Distribution, availability, and sources of trace metals in different particle size fractions of urban soils in Hong Kong: Implications for assessing the risk to human health. Environ. Pollut. 159(5), 1317-1326. https://doi.org/10.1016/j.envpol.2011.01.013.

McGill, W.B., Cole, C.V., 1981. Comparative aspects of cycling of organic C, N, S and P through soil organic matter. Geoderma 26(4), 267-286. https://doi.org/10.1016/0016-7061(81)90024-0.

Morshedizad, M., Leinweber, P., 2017. Leaching of phosphorus and cadmium in soils amended with different bone chars. Clean-Soil Air Water 45(8), 7. https://doi.org/10.1002/clen.201600635.

Morshedizad, M., Panten, K., Klysubun, W., Leinweber, P., 2018. Bone char effects on soil: Sequential fractionations and XANES spectroscopy. Soil 4(1), 23-35. https://doi.org/10.5194/soil-4-23-2018.

Nagul, E.A., McKelvie, I.D., Worsfold, P., Kolev, S.D., 2015. The molybdenum blue reaction for the determination of orthophosphate revisited: Opening the black box. Anal. Chim. Acta. 890, 60-82. https://doi.org/10.1016/j.aca.2015.07.030.

Negassa, W., Kruse, J., Michalik, D., Appathurai, N., Zuin, L., Leinweber, P., 2010. Phosphorus speciation in agro-industrial byproducts: Sequential fractionation, solution (31)P NMR, and P K- and L(2,3)-edge XANES spectroscopy. Environ. Sci. Technol. 44(6), 2092-2097. https://doi.org/10.1021/es902963c.

Obersteiner, M., Peñuelas, J., Ciais, P., van der Velde, M., Janssens, I.A., 2013. The phosphorus trilemma. Nat. Geosci. 6(11), 897-898. https://doi.org/10.1038/ngeo1990.

Panten, K., Leinweber, P., 2020. Agronomic evaluation of bone char as phosphorus fertiliser after five years of consecutive application. J. Clultivated Plants 72(12), 561-576. https://doi.org/10.5073/JfK.2020.12.02.

Paul, B.K., Vanlauwe, B., Ayuke, F., Gassner, A., Hoogmoed, M., Hurisso, T.T., Koala, S., Lelei, D., Ndabamenye, T., Six, J., Pulleman, M.M., 2013. Medium-term impact of tillage and residue management on soil aggregate stability, soil carbon and crop productivity. Agr. Ecosyst. Environ. 164, 14-22. https://doi.org/10.1016/j.agee.2012.10.003.

R Core Team, 2021. R: A language and environment for statistical computing. R Foundation for Statistical Computing, Vienna, Austria.

Ranatunga, T.D., Reddy, S.S., Taylor, R.W., 2013. Phosphorus distribution in soil aggregate size fractions in a poultry litter applied soil and potential environmental impacts. Geoderma 192, 446-452. https://doi.org/10.1016/j.geoderma.2012.08.026.

Roberts, T.L., Johnston, A.E., 2015. Phosphorus use efficiency and management in agriculture. Resour. Conserv. Recycl. 105, 275-281. https://doi.org/10.1016/j.resconrec.2015.09.013.

Santner, J., Smolders, E., Wenzel, W.W., Degryse, F., 2012. First observation of diffusion-limited plant root phosphorus uptake from nutrient solution. Plant Cell Environ. 35(9), 1558-1566. https://doi.org/10.1111/j.1365-3040.2012.02509.x.

Schmitt, D., Pagliari, P.H., do Nascimento, C.A.C., 2017. Chemical distribution of phosphorus in soils used during the development of sorption isotherms. Soil Sci. Soc. Am. J. 81(1), 84-93. https://doi.org/10.2136/sssaj2016.07.0220.

Scholz, R.W., Ulrich, A.E., Eilitta, M., Roy, A., 2013. Sustainable use of phosphorus: A finite resource. Sci. Total Environ. 461, 799-803. https://doi.org/10.1016/j.scitotenv.2013.05.043.

Siebers, N., Bauke, S.L., Tamburini, F., Amelung, W., 2018. Short-term impacts of forest clear-cut on P accessibility in soil microaggregates: An oxygen isotope study. Geoderma 315, 59-64. https://doi.org/10.1016/j.geoderma.2017.11.024.

Siebers, N., Godlinski, F., Leinweber, P., 2014. Bone char as phosphorus fertilizer involved in cadmium immobilization in lettuce, wheat, and potato cropping. J. Plant Nutr. Soil Sci. 177(1), 75-83. https://doi.org/10.1002/jpln.201300113.

Siebers, N., Kruse, J., Jia, Y.S., Lennartz, B., Koch, S., 2023. Loss of subsurface particulate and truly dissolved phosphorus during various flow conditions along a tile drain-ditch-brook continuum. Sci. Total Environ. 866, 161439. https://doi.org/10.1016/j.scitotenv.2023.161439.

Siebers, N., Kruse, J., Leinweber, P., 2013. Speciation of phosphorus and cadmium in a contaminated soil amended with bone char: Sequential fractionations and XANES spectroscopy. Water Air Soil Poll. 224(5). https://doi.org/10.1007/s11270-013-1564-7.

Siebers, N., Leinweber, P., 2013. Bone char: A clean and renewable phosphorus fertilizer with cadmium immobilization capability. J. Environ. Qual. 42(2), 405-411. https://doi.org/10.2134/jeq2012.0363.

Siebers, N., Wang, L., Funk, T., von Tucher, S., Merbach, I., Schweitzer, K., Kruse, J., 2021. Subsoils—a sink for excess fertilizer P but a minor contribution to P plant nutrition: evidence from long-term fertilization trials. Environ. Sci. Eur. 33, 60. https://doi.org/10.1186/s12302-021-00496-w.

Sinaj, S., Frossard, E., Fardeau, J.C., 1997. Isotopically exchangeable phosphate in size fractionated and unfractionated soils. Soil Sci. Soc. Am. J. 61(5), 1413-1417. https://doi.org/10.2136/sssaj1997.03615995006100050019x.

Six, J., Bossuyt, H., Degryze, S., Denef, K., 2004. A history of research on the link between (micro)aggregates, soil biota, and soil organic matter dynamics. Soil Tillage Res. 79(1), 7-31. https://doi.org/10.1016/j.still.2004.03.008.

Six, J., Paustian, K., Elliott, E.T., Combrink, C., 2000. Soil structure and organic matter: I. distribution of aggregate-size classes and aggregate-associated carbon. Soil Sci. Soc. Am. J. 64(2), 681-689. https://doi.org/10.2136/sssaj2000.642681x.

Spohn, M., Giani, L., 2011. Impacts of land use change on soil aggregation and aggregate stabilizing compounds as dependent on time. Soil Biol. Biochem. 43(5), 1081-1088. https://doi.org/10.1016/j.soilbio.2011.01.029.

Tang, Z.Y., Wu, L.H., Luo, Y.M., Christie, P., 2009. Size fractionation and characterization of nanocolloidal particles in soils. Environ. Geochem. Health 31(1), 1-10. https://doi.org/10.1007/s10653-008-9131-7.

Tisdall, J.M., Oades, J.M., 1982. Organic matter and water-stable aggregates in soils. J. Soil Sci. 33(2), 141-163. https://doi.org/10.1111/j.1365-2389.1982.tb01755.x.

Totsche, K.U., Amelung, W., Gerzabek, M.H., Guggenberger, G., Klumpp, E., Knief, C., Lehndorff, E., Mikutta, R., Peth, S., Prechtel, A., Ray, N., Kögel-Knabner, I., 2018. Microaggregates in soils. J. Plant Nutr. Soil Sci. 181(1), 104-136. https://doi.org/10.1002/jpln.201600451.

Vance, C.P., Uhde-Stone, C., Allan, D.L., 2003. Phosphorus acquisition and use: Critical adaptations by plants for securing a nonrenewable resource. New Phytol. 157(3), 423-447. https://doi.org/10.1046/j.1469-8137.2003.00695.x.

Vogel, T., Kruse, J., Siebers, N., Nelles, M., Eichler-Lobermann, B., 2017. Recycled products from municipal wastewater: Composition and effects on phosphorus mobility in a sandy soil. J. Environ. Qual. 46(2), 443-451. https://doi.org/10.2134/jeq2016.10.0392.

Vogeler, I., Rogasik, J., Funder, U., Panten, K., Schnug, E., 2009. Effect of tillage systems and P-fertilization on soil physical and chemical properties, crop yield and nutrient uptake. Soil Tillage Res. 103, 137-143. https://doi.org/10.1016/j.still.2008.10.004.

Wagener, S., Jungnickel, H., Dommershausen, N., Fischer, T., Laux, P., Luch, A., 2019. Determination of nanoparticle uptake, distribution, and characterization in plant root tissue after realistic long-term exposure to sewage sludge using information from Mass Spectrometry. Environ. Sci. Technol. 53(9), 5416-5426. https://doi.org/10.1021/acs.est.8b07222.

Wan, W.J., Li, X., Han, S., Wang, L., Luo, X.S., Chen, W.L., Huang, Q.Y., 2020. Soil aggregate fractionation and phosphorus fraction driven by long-term fertilization regimes affect the abundance and composition of P-cycling-related bacteria. Soil Tillage Res. 196. https://doi.org/10.1016/j.still.2019.104475.

Wang, J., Wu, Y., Zhou, J., Bing, H., Sun, H., Luo, J., Pu, S., 2020. Air-drying changes the distribution of Hedley phosphorus pools in forest soils. Pedosphere 30(2), 272-284. https://doi.org/10.1016/s1002-0160(17)60456-9.

Wang, X., Yost, R.S., Linquist, B.A., 2001. Soil aggregate size affects phosphorus desorption from highly weathered soils and plant growth. Soil Sci. Soc. Am. J. 65(1), 139-146. https://doi.org/10.2136/sssaj2001.651139x.

Warren, G.P., Robinson, J.S., Someus, E., 2008. Dissolution of phosphorus from animal bone char in 12 soils. Nutr. Cycl. Agroecosyst. 84(2), 167-178. https://doi.org/10.1007/s10705-008-9235-6.

Wiesler, F., Appel, T., Dittert, K., Ebertseder, T., Müller, T., Nätscher, L., Olfs, H.W., Rex, M., Schweitzer, K., Steffens, D., Taube, F., Zorn, W., 2018. Phosphordungung nach Bodenuntersuchung und Pflanzenbedarf: VDLUFA-Standpunkt.

Wright, A.L., 2009. Phosphorus sequestration in soil aggregates after long-term tillage and cropping. Soil Tillage Res. 103(2), 406-411. https://doi.org/10.1016/j.still.2008.12.008.

Zhang, M.K., He, Z.L., Calvert, D.V., Stoffella, P.J., Yang, X.E., Li, Y.C., 2003. Phosphorus and heavy metal attachment and release in sandy soil aggregate fractions. Soil Sci. Soc. Am. J. 67(4), 1158-1167. https://doi.org/10.2136/sssaj2003.1158.

Zhang, Q.Q., Song, Y.F., Wu, Z., Yan, X.Y., Gunina, A., Kuzyakov, Y., Xiong, Z.Q., 2020. Effects of six-year biochar amendment on soil aggregation, crop growth, and nitrogen and phosphorus use efficiencies in a rice-wheat rotation. J. Clean. Prod. 242, 118435. https://doi.org/10.1016/j.jclepro.2019.118435.

Zimmer, D., Kruse, J., Siebers, N., Panten, K., Oelschlager, C., Warkentin, M., Hu, Y.F., Zuin, L., Leinweber, P., 2018. Bone char vs. S-enriched bone char: Multi-method characterization of bone chars and their transformation in soil. Sci. Total Environ. 643, 145-156. https://doi.org/10.1016/j.scitotenv.2018.06.076.

Zimmer, D., Panten, K., Frank, M., Springer, A., Leinweber, P., 2019. Sulfur-enriched bone char as alternative P fertilizer: Spectroscopic, wet chemical, and yield response evaluation. Agriculture 9(1), 21. https://doi.org/10.3390/agriculture9010021.
Zwetsloot, M.J., Lehmann, J., Bauerle, T., Vanek, S., Hestrin, R., Nigussie, A., 2016. Phosphorus availability from bone char in a P-fixing soil influenced by root-mycorrhizae-biochar interactions. Plant Soil 408(1-2), 95-105. https://doi.org/10.1007/s11104-016-2905-2.
Zwetsloot, M.J., Lehmann, J., Solomon, D., 2015. Recycling slaughterhouse waste into fertilizer: How do pyrolysis temperature and biomass additions affect phosphorus availability and chemistry? J. Sci. Food Agric. 95(2), 281-288. https://doi.org/10.1002/jsfa.6716.

Figures & captions

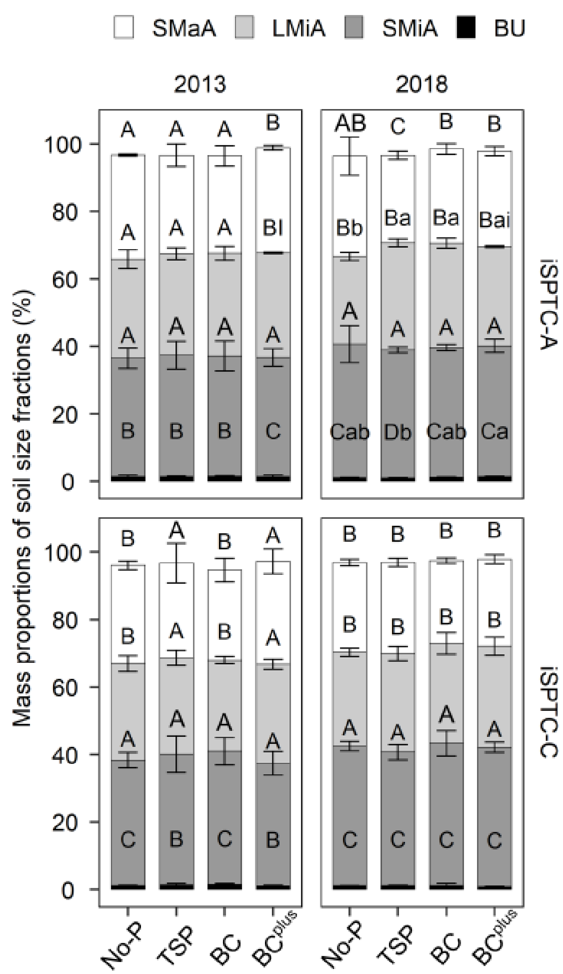

Figure 1. Mass proportions of soil size fractions (small macroaggregates, SMaA (250 to 2000 µm); large microaggregates, LMiA (53 to 250 µm); small microaggregates, SMiA (1 to 53 µm); and building units, BU (< 1 µm)) for four treatments (No phosphorus, No-P; triple superphosphate, TSP;

bone char, BC; and sulfur modified bone char, BC^{plus}) in severely deficient or sufficient initial soil test P class (iSPTC-A or -C) soil before the start of the field trial (2013) and after 5 years (2018). Significant differences between soil size fractions within a treatment in a year were labeled with different capital letters; between treatments within a soil size fraction in a year were labeled with different lowercase letters; between years within a soil size fraction and a treatment were labeled with i or I, respectively. The value labelled with “I” was tested significantly higher than the value labelled with “i”. n = 3.

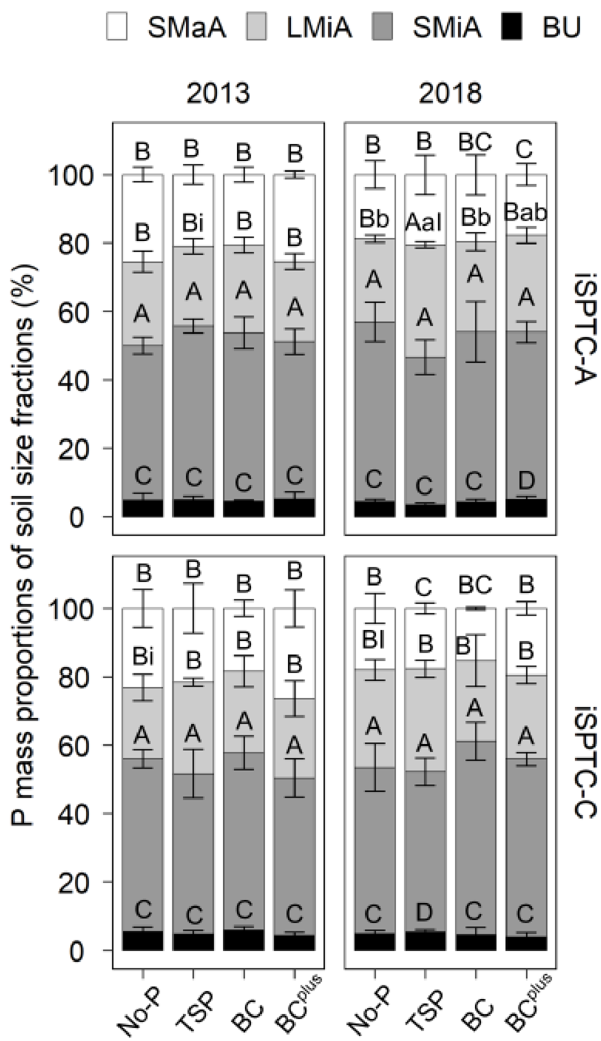

Figure 2. Proportions of total extracted P (mg kg^{-1} bulk soil) in each soil size fraction (small macroaggregates, SMaA (250 to 2000 µm); large microaggregates, LMiA (53 to 250 µm); small microaggregates, SMiA (1 to 53 µm); and building units, BU (< 1 µm)) to sum of total extracted P of four soil size fractions under different treatments (No phosphorus, No-P; triple superphosphate, TSP; bone char, BC; and sulfur modified bone

char, BC^{plus}) in severely deficient or sufficient initial soil test P class (iSPTC-A or -C) soil. Significant differences between soil size fractions within a treatment in a year were labeled with different capital letters; between treatments within a soil size fraction in one year were labeled with different lowercase letters; between years within a soil size fraction and a treatment were labeled with i or I, respectively. The value labelled with “I” was tested significantly higher than the value labelled with “i”. n = 3.

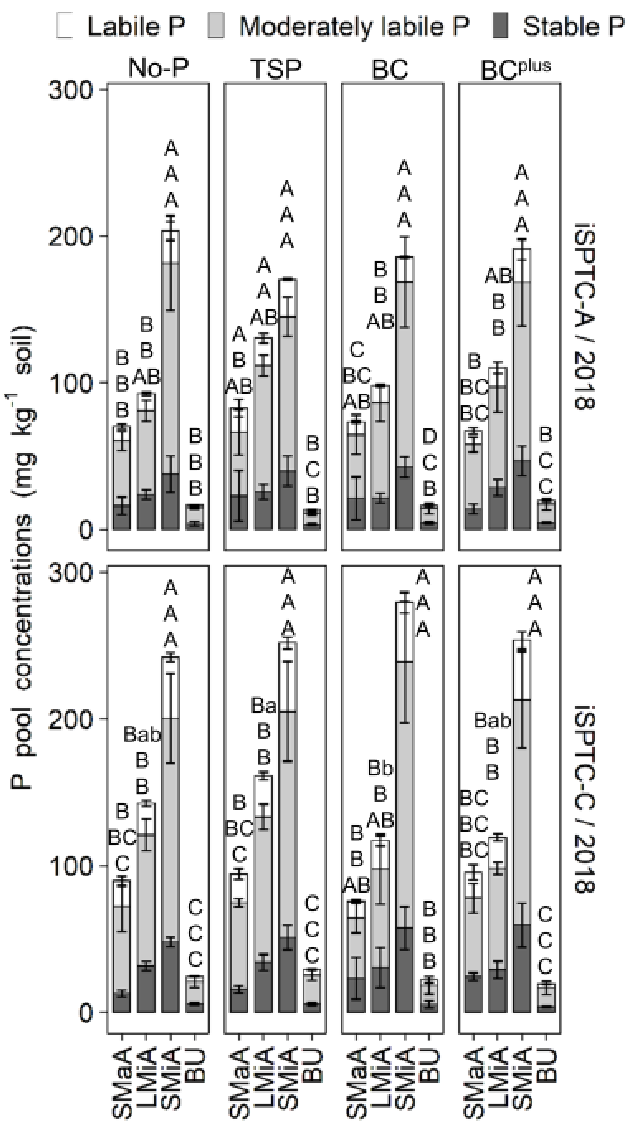

514 **Figure 3.** Labile (sum of H_2O-P_i, H_2O-P_o, $NaHCO_3$-P_i and $NaHCO_3$-P_o), moderately labile (NaOH-P_i and NaOH-P_o) and stable (H_2SO_4-P) P pool

515 concentrations (mg P kg^{-1} soil) in soil size fractions (small macroaggregates, SMaA (250 to 2000 µm); large microaggregates, LMiA (53 to 250 µm);

small microaggregates, SMiA (1 to 53 µm); and building units, BU (< 1 µm)) and treatments (No phosphorus, No-P; triple superphosphate, TSP; bone char, BC; and sulfur modified bone char, BC^{plus}) in severely deficient or sufficient initial soil test P class (iSPTC-A or -C) soil. Significant differences between soil size fractions within a treatment at each soil P class were labeled with different capital letters; between treatments for a soil size fraction at each soil P class were labeled with different lowercase letters. n = 3. Significance labels were above each bar of the plot and from top to down were for labile, moderately labile and stable P, respectively.

Supplementary data

Table S1

Elemental concentrations of soil size fractions (SMaA, LMiA, SMiA and BU) and bulk soil pH of treatments (No-P, TSP, BC and BC^{plus}) at year 2013 and year 2018 in iSPTC-A soil.

Treatment	Size fraction	Bulk soil pH ($CaCl_2$)		C (g kg^{-1} fraction)		N (g kg^{-1} fraction)		S (mg kg^{-1} fraction)	
		Before start (2013)	2018	Before start (2013)	2018	Before start (2013)	2018	Before start (2013)	2018
No-P	SMaA	5.1±0.1	5.9±0.3	10.2±1.4^{C}	10.0±1.3^{C}	0.53±0.05^{C}	0.56±0.05^{C}	120±10^{B}	117±28^{B}
	LMiA			11.8±0.5^{BC}	12.4±1.3^{BC}	0.74±0.02^{BC}	0.78±0.07^{B}	137±22^{B}	145±12^{B}
	SMiA			13.8±0.8^{B}	14.0±0.4^{B}	0.97±0.05^{B}	0.95±0.03^{B}	168±24^{B}	178±4^{B}
	BU			47.9±1.7^{A}	46.4±0.4^{A}	3.75±0.21^{A}	3.61±0.08^{A}	673±59^{A}	772±44^{A}
TSP	SMaA	5.2±0.1^{i}	6.0±0.3^{I}	10.4±1.0^{B}	10.1±1.9^{B}	0.58±0.05^{B}	0.56±0.10^{B}	124±11^{B}	144±14^{B}
	LMiA			11.3±1.1^{B}	12.6±1.4^{B}	0.71±0.07^{B}	0.83±0.11^{B}	138±10^{B}	169±14^{B}
	SMiA			13.0±0.9^{B}	13.6±1.0^{B}	0.90±0.09^{B}	0.93±0.10^{B}	169±6^{B}	183±7^{B}
	BU			48.1±10.1^{A}	48.9±3.9^{A}	3.72±0.77^{A}	3.85±0.33^{A}	700±251^{A}	846±149^{A}
BC	SMaA	5.1±0.1^{i}	6.0±0.1^{I}	9.5±0.9^{B}	8.6±1.4^{B}	0.53±0.05^{B}	0.55±0.09^{B}	116±8^{B}	131±11^{B}
	LMiA			11.3±1.1^{B}	11.8±0.7^{B}	0.72±0.06^{B}	0.79±0.05^{B}	134±14^{B}	152±6^{B}
	SMiA			12.7±0.5^{B}	14.1±0.6^{B}	0.89±0.06^{B}	0.99±0.06^{B}	164±12^{B}	193±15^{B}
	BU			44.1±4.0^{A}	57.4±6.8^{A}	3.44±0.34^{A}	4.20±0.84^{A}	597±119^{A}	1205±253^{A}
BC^{plus}	SMaA	5.2±0.1^{i}	6.0±0.2^{I}	11.1±0.4^{B}	8.6±1.6^{B}	0.58±0.04^{B}	0.49±0.08^{B}	128±7^{B}	134±17^{B}
	LMiA			11.7±0.6^{B}	11.6±0.7^{B}	0.74±0.03^{B}	0.73±0.05^{B}	141±19^{B}	151±6^{B}
	SMiA			14.0±0.7^{B}	13.5±0.5^{B}	0.99±0.05^{B}	0.90±0.04^{B}	173±20^{B}	186±10^{B}
	BU			52.0±6.4^{A}	48.8±11.9^{A}	4.02±0.51^{A}	3.68±1.03^{A}	777±168^{A}	889±137^{A}

Table S1 (continued)

Treatment	Size fraction	P		Ca		Fe		Mg	
		g kg^{-1} fraction							
		Before start (2013)	2018	Before start (2013)	2018	Before start (2013)	2018	Before start (2013)	2018
No-P	SMaA	0.33±0.07^{B}	0.24±0.04^{C}	0.72±0.14^{B}	1.07±0.34^{C}	5.6±0.8^{C}	6.2±0.7^{B}	0.41±0.05^{C}	0.48±0.03^{C}
	LMiA	0.33±0.03^{B}	0.36±0.05^{C}	0.96±0.16^{B}	1.33±0.23^{BC}	7.0±0.3^{C}	7.7±0.4^{B}	0.62±0.02^{C}	0.68±0.04^{C}
	SMiA	0.52±0.13^{B}	0.51±0.07^{B}	1.32±0.20^{Bi}	2.06±0.23^{BI}	9.6±0.5^{BC}	11.8±1.1^{B}	0.95±0.08^{B}	1.20±0.09^{B}
	BU	1.36±0.19^{A}	1.56±0.03^{A}	3.81±0.48^{A}	4.72±0.49^{A}	28.9±2.5^{A}	25.3±3.8^{A}	3.07±0.15^{A}	3.02±0.14^{A}
TSP	SMaA	0.26±0.02^{B}	0.32±0.10^{B}	0.80±0.15^{C}	1.12±0.26^{C}	6.2±0.2^{B}	5.6±0.6^{C}	0.49±0.06^{C}	0.50±0.07^{C}
	LMiA	0.28±0.05^{B}	0.41±0.03^{B}	0.89±0.02^{BCi}	1.45±0.09^{BCI}	6.6±0.2^{B}	7.5±0.5^{BC}	0.61±0.01^{BC}	0.69±0.02^{BC}
	SMiA	0.52±0.06^{B}	0.45±0.02^{B}	1.32±0.11^{Bi}	1.88±0.16^{BI}	9.4±0.4^{B}	9.8±0.1^{B}	0.96±0.04^{B}	0.99±0.06^{B}
	BU	1.38±0.43^{A}	1.47±0.07^{A}	3.75±0.27^{Ai}	5.18±0.23^{AI}	26.9±5.5^{A}	25.3±2.9^{A}	3.13±0.26^{A}	2.98±0.21^{A}
BC	SMaA	0.26±0.02^{C}	0.26±0.08^{B}	0.66±0.09^{Ci}	1.02±0.04^{BI}	5.8±0.8^{B}	7.1±1.1^{B}	0.43±0.04^{C}	0.54±0.16^{B}
	LMiA	0.31±0.03^{C}	0.32±0.06^{B}	0.86±0.07^{C}	1.40±0.30^{B}	6.8±0.0^{B}	7.6±0.8^{B}	0.60±0.01^{C}	0.70±0.08^{B}
	SMiA	0.51±0.06^{B}	0.48±0.09^{B}	1.24±0.15^{B}	1.74±0.50^{B}	9.4±0.4^{B}	9.7±1.8^{B}	0.94±0.05^{B}	0.94±0.22^{B}
	BU	1.12±0.11^{A}	1.35±0.28^{A}	3.51±0.18^{A}	5.18±0.61^{A}	26.1±4.3^{A}	35.4±0.4^{A}	3.04±0.13^{A}	3.37±0.33^{A}
BC^{plus}	SMaA	0.33±0.07^{B}	0.24±0.01^{B}	0.86±0.10^{C}	0.87±0.26^{B}	6.0±0.4^{B}	4.7±1.3^{B}	0.47±0.09^{C}	0.38±0.13^{B}
	LMiA	0.31±0.07^{Bi}	0.37±0.08^{BI}	0.99±0.10^{C}	1.40±0.32^{B}	6.9±0.5^{B}	7.2±1.3^{B}	0.62±0.02^{BC}	0.66±0.11^{B}
	SMiA	0.53±0.13^{B}	0.49±0.11^{B}	1.40±0.11^{B}	1.89±0.30^{B}	9.6±0.6^{B}	10.0±0.7^{B}	0.97±0.07^{B}	0.98±0.08^{B}
	BU	1.59±0.27^{A}	1.49±0.47^{A}	4.05±0.22^{A}	4.38±1.12^{A}	29.6±3.6^{A}	25.5±7.6^{A}	3.16±0.26^{A}	2.89±0.49^{A}

SMaA = small macroaggregate. LMiA = large microaggregate. SMiA = small microaggregate. BU = building units. TSP = triple superphosphate. BC = bone char. BC^{plus} = sulfur modified bone char. The pH values were measured with bulk soil samples of each treatment.

Significant differences between size fractions within a treatment in the same year were labeled with different capital letters; between four treatments within an aggregate size fraction in the same year were labeled with different lowercase letters; between years within a size fraction and a treatment were labeled with i or I, respectively. The value labelled with “I” was tested significantly higher than value labelled with “i”. Values were mean ± standard deviation (n = 3).

Table S2

Elemental concentrations of soil size fractions (SMaA, LMiA, SMiA and BU) and bulk soil pH of treatments (No-P, TSP, BC and BC^{plus}) at year 2013 and year 2018 in iSPTC-C soil.

Treatment	Size fraction	Bulk soil pH ($CaCl_2$)		C (g kg^{-1} fraction)		N (g kg^{-1} fraction)		S (mg kg^{-1} fraction)	
		Before start (2013)	2018	Before start (2013)	2018	Before start (2013)	2018	Before start (2013)	2018
No-P	SMaA	5.2±0.1^{i}	5.9±0.2^{I}	10.8±1.0^{B}	10.4±0.3^{B}	0.58±0.05^{C}	0.59±0.03^{B}	123±10^{B}	113±26^{B}
	LMiA			12.0±0.6^{B}	12.6±0.0^{B}	0.75±0.06^{BC}	0.80±0.00^{B}	141±11^{B}	136±20^{B}
	SMiA			13.8±0.6^{B}	14.1±1.2^{B}	0.94±0.05^{B}	1.00±0.08^{B}	169±12^{B}	175±12^{Bab}
	BU			54.2±2.0^{A}	49.6±4.2^{A}	4.20±0.23^{A}	3.76±0.28^{A}	753±80^{A}	779±47^{A}
TSP	SMaA	5.2±0.0^{i}	6.1±0.2^{I}	10.5±1.2^{B}	11.1±1.1^{C}	0.57±0.04^{B}	0.61±0.05^{C}	127±18^{B}	148±9^{BC}
	LMiA			12.7±0.4^{B}	13.1±0.5^{BC}	0.81±0.03^{B}	0.85±0.01^{B}	150±19^{B}	122±8^{C}
	SMiA			13.8±0.8^{B}	14.7±0.8^{B}	0.97±0.09^{B}	1.01±0.03^{B}	169±12^{B}	167±21^{Bb}
	BU			47.9±5.8^{A}	47.3±0.7^{A}	3.58±0.49^{A}	3.69±0.11^{A}	807±215^{A}	717±11^{A}
BC	SMaA	5.2±0.0^{i}	6.0±0.3^{I}	10.0±0.5^{B}	9.0±1.9^{B}	0.54±0.01^{B}	0.49±0.08^{B}	121±9^{B}	127±20^{B}
	LMiA			12.1±0.8^{B}	11.6±2.4^{B}	0.75±0.07^{B}	0.76±0.14^{B}	142±21^{B}	148±31^{B}
	SMiA			13.4±0.6^{B}	15.0±1.2^{B}	0.93±0.08^{Bi}	1.04±0.08^{BI}	161±10^{Bi}	205±5^{BaI}
	BU			48.3±6.6^{A}	59.5±15.8^{A}	3.60±0.53^{A}	4.75±0.93^{A}	790±217^{Ai}	1124±250^{AI}
BC^{plus}	SMaA	5.2±0.1	5.8±0.4	11.3±0.9^{C}	10.6±1.0^{C}	0.61±0.04^{C}	0.56±0.06^{C}	129±17^{Bi}	145±11^{BI}
	LMiA			12.6±0.3^{BC}	10.6±0.7^{C}	0.81±0.03^{BCI}	0.66±0.06^{Ci}	150±7^{B}	172±42^{B}
	SMiA			14.2±0.1^{B}	14.7±0.3^{B}	0.99±0.03^{B}	0.97±0.04^{B}	176±5^{Bi}	199±3^{BabI}
	BU			53.7±1.6^{A}	54.2±0.5^{A}	4.17±0.23^{A}	4.21±0.08^{A}	770±87^{A}	983±188^{A}

Table S2 (continued)

Treatment	Size fraction	P		Ca		Fe		Mg	
		g kg^{-1} fraction							
		Before start (2013)	2018	Before start (2013)	2018	Before start (2013)	2018	Before start (2013)	2018
No-P	SMaA	0.45±0.13^{B}	0.33±0.07^{B}	0.78±0.02^{B}	1.21±0.30^{B}	5.3±0.9^{B}	5.8±0.7^{B}	0.40±0.03^{C}	0.55±0.15^{C}
	LMiA	0.40±0.06^{Bi}	0.51±0.04^{BI}	1.02±0.10^{B}	1.34±0.19^{B}	6.5±0.5^{B}	7.0±0.1^{B}	0.59±0.03^{C}	0.65±0.02^{C}
	SMiA	0.76±0.07^{B}	0.58±0.07^{B}	1.40±0.07^{B}	1.66±0.22^{B}	9.2±0.1^{B}	9.1±0.3^{B}	0.90±0.03^{B}	0.92±0.04^{B}
	BU	2.58±0.56^{AI}	2.11±0.52^{Ai}	4.71±0.50^{A}	5.12±0.59^{A}	33.9±2.1^{AI}	25.2±3.1^{Ai}	3.28±0.17^{A}	2.89±0.09^{Aab}
TSP	SMaA	0.40±0.04^{C}	0.35±0.00^{C}	0.84±0.09^{B}	1.26±0.36^{B}	6.0±0.6^{B}	6.4±0.7^{C}	0.44±0.08^{C}	0.46±0.07^{D}
	LMiA	0.51±0.05^{BC}	0.55±0.03^{B}	1.15±0.06^{B}	1.69±0.29^{B}	7.1±0.3^{B}	7.5±0.1^{C}	0.62±0.03^{C}	0.67±0.01^{C}
	SMiA	0.65±0.06^{B}	0.64±0.06^{B}	1.51±0.04^{B}	2.19±0.25^{B}	9.7±0.4^{B}	10.2±0.3^{B}	0.93±0.01^{B}	1.02±0.04^{B}
	BU	1.91±0.13^{Ai}	2.43±0.09^{AI}	4.51±0.60^{A}	5.15±0.66^{A}	27.6±4.4^{A}	23.0±0.4^{A}	2.93±0.16^{A}	2.81±0.03^{Ab}
BC	SMaA	0.37±0.03^{B}	0.31±0.01^{B}	0.79±0.03^{C}	1.56±0.61^{B}	5.6±0.6^{B}	5.6±0.1^{B}	0.40±0.04^{C}	0.54±0.22^{B}
	LMiA	0.47±0.08^{B}	0.39±0.12^{B}	1.07±0.01^{BCi}	1.72±0.05^{BI}	6.6±0.9^{B}	8.1±0.4^{B}	0.60±0.04^{Ci}	0.76±0.02^{BI}
	SMiA	0.71±0.11^{B}	0.67±0.11^{B}	1.48±0.04^{Bi}	2.25±0.12^{BI}	9.4±0.4^{B}	10.6±1.4^{B}	0.91±0.04^{B}	1.06±0.12^{B}
	BU	2.30±0.76^{A}	2.05±0.38^{A}	4.37±0.38^{A}	6.78±1.37^{A}	28.4±5.1^{A}	30.8±7.1^{A}	2.99±0.19^{A}	3.42±0.33^{Aa}
BC^{plus}	SMaA	0.48±0.10^{B}	0.37±0.05^{B}	0.83±0.09^{B}	1.51±0.19^{B}	5.7±1.1^{B}	6.7±1.2^{B}	0.44±0.07^{C}	0.42±0.05^{C}
	LMiA	0.43±0.08^{B}	0.40±0.01^{B}	1.10±0.10^{B}	1.36±0.48^{B}	7.0±0.4^{B}	6.9±1.5^{B}	0.62±0.02^{BC}	0.62±0.15^{BC}
	SMiA	0.70±0.07^{B}	0.61±0.06^{B}	1.44±0.12^{B}	1.79±0.23^{B}	9.5±0.4^{B}	9.8±0.3^{B}	0.92±0.01^{B}	0.95±0.04^{B}
	BU	2.19±0.30^{A}	2.26±0.18^{A}	4.85±0.56^{A}	5.31±0.60^{A}	33.1±3.5^{A}	27.4±4.1^{A}	3.22±0.25^{A}	2.93±0.21^{Aab}

SMaA = small macroaggregate. LMiA = large microaggregate. SMiA = small microaggregate. BU = building units. TSP = triple superphosphate. BC = bone char. BC^{plus} = sulfur modified bone char. The pH values were measured with bulk soil samples of each treatment.

Significant differences between size fractions within a treatment in the same year were labeled with different capital letters; between four treatments within an aggregate size fraction in the same year were labeled with different lowercase letters; between years within a size fraction and a treatment were labeled with i or I, respectively. The value labelled with "I" was tested significantly higher than value labelled with "i". Values were mean ± standard deviation (n = 3).

Table S3

Phosphorus concentrations (mg kg^{-1} fraction) of P fractions in soil size fractions (SMaA, LMiA, SMiA and BU) of treatments (No-P, TSP, BC and BC^{plus}) at year 2013 and year 2018 in iSPTC-A soil.

Treatment	Size fraction	H_2O-P_i		H_2O-P_o		$NaHCO_3$-P_i		$NaHCO_3$-P_o
		mg kg^{-1} fraction (%)						
		Before start (2013)	2018	Before start (2013)	2018	Before start (2013)	2018	Before start (2013)
No-P	SMaA	6.8±5.8^{AB} (1.9)	3.7±0.4 (1.6)	24±26 (6)	7±3^{B} (3^{A})	13±3^{C} (4)	13±5^{C} (5)	15±3^{BI} (5^{B})
	LMiA	6.4±2.8^{AB} (1.9)	4.4±3.3 (1.2)	3±1 (1)	7±2^{B} (2^{AB})	27±8^{B} (8)	19±5^{C} (5)	10±3^{B} (3^{B})
	SMiA	5.0±2.8^{B} (1.0)	5.5±1.4 (1.1^{ab})	4±2^{I} (1)	2±1^{Ci} (0^{Bb})	31±8^{B} (6)	31±7^{B} (6)	16±2^{B} (3^{B})
	BU	13.4±5.9^{A} (1.0)	7.4±6.4 (0.5)	7±14 (0)	13±2^{A} (1^{AB})	71±20^{A} (4)	63±13^{Ab} (4)	110±18^{AI} (8^{A})
TSP	SMaA	10.0±8.9 (3.7)	8.9±2.3 (3.0^{A})	29±24^{A} (11)	24±25 (8)	10±1^{C} (4)	18±5^{C} (6)	12±1^{B} (5^{AB})
	LMiA	4.8±1.7 (1.7)	8.5±2.0 (2.1^{AB})	3±4^{B} (1)	9±8 (2)	13±4^{Ci} (5^{i})	29±7^{BI} (7^{I})	14±3^{B} (5^{AB})
	SMiA	2.9±1.2^{i} (0.6^{i})	8.8±0.4^{I} (2.0^{ABaI})	2±1^{Bi} (0^{i})	6±1^{I} (1^{aI})	23±3^{Bi} (4^{i})	37±2^{BI} (8^{I})	13±2^{B} (2^{B})
	BU	7.9±3.9 (0.6)	10.2±1.8 (0.7^{B})	14±6^{AB} (1)	12±3 (1)	50±10^{Ai} (3)	98±9^{AaI} (5)	78±16^{Ai} (6^{A})
BC	SMaA	8.5±10.1 (3.1)	2.8±2.0 (1.0^{AB})	22±27 (8)	7±2^{A} (3)	10±1^{C} (4^{AB})	11±5^{C} (4)	12±0^{B} (5^{AB})
	LMiA	4.3±1.9 (1.4)	4.5±0.9 (1.5^{A})	4±3 (1)	3±1^{B} (1)	17±2^{BC} (5^{A})	23±6^{B} (8)	12±0^{B} (4^{AB})
	SMiA	2.2±0.6 (0.4)	2.5±0.9 (0.5^{ABb})	4±2 (1)	2±1^{B} (1^{b})	22±1^{B} (4^{AB})	24±1^{B} (5)	14±3^{B} (3^{B})
	BU	10.9±8.3 (0.9)	3.2±2.4 (0.2^{B})	4±10 (0)	7±1^{A} (0)	50±10^{Ai} (4^{B})	65±6^{AabI} (4)	85±28^{A} (7^{A})
BC^{plus}	SMaA	8.3±4.4^{AB} (2.4^{A})	4.9±1.2 (2.1)	31±22^{A} (9^{A})	6±3^{B} (2^{A})	13±4^{C} (4)	13±3^{B} (6)	16±2^{BI} (5)
	LMiA	6.8±2.1^{AB} (2.2^{A})	6.1±3.7 (1.6)	2±1^{B} (1^{B})	2±1^{B} (1^{B})	24±13^{BC} (7)	25±13^{B} (7)	11±5^{B} (4)
	SMiA	5.7±1.7^{B} (1.1^{AB})	6.8±3.7 (1.3^{ab})	2±2^{B} (0^{B})	3±1^{B} (1^{Bab})	32±6^{B} (6)	33±10^{B} (7)	15±3^{B} (3)
	BU	10.4±1.9^{A} (0.7^{B})	5.7±4.5 (0.3)	17±7^{AB} (1^{B})	12±5^{A} (1^{B})	71±20^{A} (4)	85±35^{Aab} (5)	103±18^{A} (7)

Table S3 (continued)

Treatment	Size fraction	$NaHCO_3$-P_o	$NaOH$-P_i		$NaOH$-P_o		H_2SO_4-P	
		mg kg^{-1} fraction (%)						
		2018	Before start (2013)	2018	Before start (2013)	2018	Before start (2013)	2018
No-P	SMaA	10±3^{Bi} (4)	56±14^{C} (17)	52±14^{D} (21^{AB})	143±23^{C} (45)	99±11^{B} (42)	72±55^{B} (20)	58±32^{B} (23)
	LMiA	14±4^{B} (4)	80±14^{BC} (24)	75±16^{C} (21^{AB})	137±28^{C} (42)	146±20^{B} (41)	67±13^{B} (20^{i})	92±16^{B} (26^{abI})
	SMiA	16±1^{B} (3)	109±26^{B} (22)	126±19^{B} (25^{A})	241±88^{B} (46)	235±24^{B} (46)	114±50^{B} (22)	94±21^{B} (18)
	BU	82±9^{Ai} (5)	383±51^{Aa} (23)	318±20^{A} (18^{B})	430±22^{A} (27)	735±162^{A} (41)	349±137^{A} (21)	337±105^{A} (19)
TSP	SMaA	12±0^{B} (4^{B})	50±9^{C} (19)	58±14^{C} (19^{B})	111±12^{B} (43^{ABI})	107±41^{B} (34^{ABi})	40±10^{B} (15)	88±63^{B} (26)
	LMiA	13±3^{B} (3^{B})	66±7^{BC} (24)	90±10^{C} (22^{B})	118±25^{B} (41^{AB})	181±18^{B} (44^{A})	64±28^{B} (22)	81±17^{B} (19^{b})
	SMiA	15±1^{B} (3^{B})	90±12^{B} (17^{i})	127±10^{B} (28^{AI})	297±49^{AB} (57^{A})	150±42^{B} (33^{AB})	90±3^{B} (17)	104±25^{B} (23)
	BU	127±15^{AI} (7^{A})	305±40^{Abi} (20)	387±32^{AI} (21^{B})	576±402^{A} (34^{B})	480±102^{A} (26^{B})	351±55^{A} (24)	359±49^{A} (20)
BC	SMaA	10±3^{B} (4^{B})	46±9^{C} (18)	47±13^{D} (18)	120±25^{C} (46^{A})	110±40^{B} (42)	42±7^{B} (16)	74±47^{B} (27)
	LMiA	7±6^{B} (2^{B})	65±6^{BC} (21)	72±1^{C} (23)	138±19^{C} (45^{AB})	138±47^{B} (43)	67±25^{B} (22)	69±13^{B} (22^{ab})
	SMiA	15±1^{B} (3^{B})	83±6^{Bi} (16)	98±2^{BI} (21)	296±50^{B} (58^{A})	230±79^{B} (47)	86±10^{B} (17^{i})	110±19^{B} (23^{I})
	BU	76±16^{A} (6^{A})	299±34^{Ab} (22)	317±30^{A} (21)	373±58^{A} (27^{B})	519±220^{A} (32)	336±74^{A} (25)	361±48^{A} (23)
BC^{plus}	SMaA	9±2^{Bi} (4^{AB})	59±9^{C} (18)	57±6^{B} (24)	135±25^{B} (42)	98±26^{B} (41)	70±57^{B} (20)	50±11^{B} (21)
	LMiA	11±5^{B} (3^{B})	82±11^{C} (27)	85±25^{B} (23)	118±32^{B} (38)	148±60^{B} (39)	64±19^{Bi} (20)	97±15^{BI} (26^{a})
	SMiA	16±3^{B} (3^{B})	117±13^{B} (23)	124±29^{B} (25)	242±89^{B} (45)	190±73^{B} (38)	119±45^{B} (22)	120±23^{B} (25)
	BU	87±27^{A} (6^{A})	389±41^{Aa} (21)	351±95^{A} (20)	634±352^{A} (33)	615±276^{A} (34)	364±126^{A} (20)	337±38^{A} (20)

Table S3 (continued)

Treatment	Size fraction	P_i		P_o		P_i / P_o	
		mg kg^{-1} fraction (%)					
		Before start (2013)	2018	Before start (2013)	2018	Before start (2013)	2018
No-P	SMaA	148 ± 65^{B} (43)	126 ± 51^{C} (51)	183 ± 13^{CI} (57)	115 ± 13^{Ci} (49)	0.8 ± 0.3	1.1 ± 0.5^{A}
	LMiA	181 ± 36^{B} (55)	190 ± 37^{BC} (53)	150 ± 29^{C} (45)	167 ± 18^{BC} (47)	1.3 ± 0.4	1.1 ± 0.1^{A}
	SMiA	260 ± 82^{B} (50)	257 ± 48^{B} (50)	261 ± 92^{B} (50)	253 ± 24^{B} (50)	1.1 ± 0.5	1.0 ± 0.1^{AB}
	BU	817 ± 181^{A} (49)	727 ± 135^{A} (41)	820 ± 40^{A} (51)	1048 ± 129^{A} (59)	1.0 ± 0.2	0.7 ± 0.2^{B}
TSP	SMaA	109 ± 10^{C} (42)	173 ± 77^{C} (54)	153 ± 19^{B} (58)	143 ± 48^{B} (46)	0.7 ± 0.1^{B}	1.3 ± 0.6^{AB}
	LMiA	148 ± 24^{BC} (52)	208 ± 32^{BC} (50)	136 ± 26^{B} (48)	203 ± 11^{B} (50)	1.1 ± 0.0^{A}	1.0 ± 0.2^{B}
	SMiA	206 ± 14^{B} (40)	277 ± 31^{B} (62)	312 ± 51^{B} (60)	171 ± 41^{B} (38)	0.7 ± 0.1^{B}	1.7 ± 0.5^{A}
	BU	714 ± 81^{Ai} (47)	853 ± 67^{AI} (47)	860 ± 443^{A} (53)	956 ± 6^{A} (53)	1.0 ± 0.4^{AB}	0.9 ± 0.1^{B}
BC	SMaA	107 ± 14^{C} (41^{AB})	135 ± 61^{C} (50)	154 ± 20^{C} (59^{AB})	127 ± 40^{B} (50)	0.7 ± 0.1^{B}	1.1 ± 0.6
	LMiA	153 ± 18^{BC} (50^{AB})	169 ± 7^{C} (54)	155 ± 21^{C} (50^{AB})	149 ± 54^{B} (46)	1.0 ± 0.1^{A}	1.2 ± 0.4
	SMiA	192 ± 15^{Bi} (38^{B})	235 ± 19^{BI} (50)	313 ± 50^{B} (62^{A})	247 ± 77^{B} (50)	0.6 ± 0.1^{B}	1.0 ± 0.3
	BU	696 ± 87^{A} (51^{A})	747 ± 62^{A} (48)	666 ± 110^{A} (49^{B})	814 ± 236^{A} (52)	1.1 ± 0.2^{A}	0.9 ± 0.2
BC^{plus}	SMaA	151 ± 62^{C} (44)	125 ± 20^{C} (53)	182 ± 15^{B} (56)	113 ± 22^{B} (47)	0.8 ± 0.3^{B}	1.2 ± 0.4
	LMiA	176 ± 44^{BCi} (57)	214 ± 51^{BCI} (57)	131 ± 29^{B} (43)	161 ± 64^{B} (43)	1.4 ± 0.3^{A}	1.5 ± 0.8
	SMiA	273 ± 63^{B} (52)	284 ± 65^{B} (58)	259 ± 91^{B} (48)	209 ± 74^{B} (42)	1.1 ± 0.5^{AB}	1.4 ± 0.5
	BU	834 ± 159^{A} (46)	778 ± 165^{A} (45)	1014 ± 310^{A} (54)	973 ± 391^{A} (55)	0.9 ± 0.3^{B}	0.8 ± 0.2

SMaA = small macroaggregate. LMiA = large microaggregate. SMiA = small microaggregate. BU = building units. TSP = triple superphosphate. BC = bone char. BC^{plus} = sulfur modified bone char. P_t = total P. P_i = total inorganic P. P_o = total organic P.

Significant differences between size fractions within a treatment in the same year were labeled with different capital letters; between four treatments within an aggregate size fraction in the same year were labeled with different lowercase letters; between years within a size fraction and a treatment were labeled with i or I, respectively. The value labelled with "I" was tested significantly higher than value labelled with "i". Values were mean ± standard deviation (n = 3). Values in brackets were proportions of each P fraction to total P in each soil size fraction.

Table S4

Phosphorus concentrations (mg kg^{-1} fraction) of P fractions in size fractions (SMaA, LMiA, SMiA and BU) of treatments (No-P, TSP, BC and BC^{plus}) at year 2013 and year 2018 in iSPTC-C soil.

Treatment	Size fraction	H_2O-P_i		H_2O-P_o		$NaHCO_3$-P_i		$NaHCO_3$-P_o	
		mg kg^{-1} fraction (%)							
		Before start (2013)	2018	Before start (2013)	2018	Before start (2013)	2018	Before start (2013)	2018
No-P	SMaA	14±1^{BI} (3^{AB})	10±2^{Ci} (3^{A})	11±4^{B} (2^{A})	16±9 (5)	36±2^{BI} (8^{AB})	24±5^{Di} (7^{AB})	21±6^{B} (5)	16±2^{B} (5)
	LMiA	16±0^{B} (4^{AI})	9±4^{Cb} (2^{ABi})	5±2^{C} (1^{AB})	7±5 (1)	51±5^{BI} (13^{AI})	40±3^{Ci} (8^{ABi})	22±4^{B} (6)	20±2^{B} (4)
	SMiA	18±3^{B} (2^{AB})	14±2^{Bb} (2^{AB})	8±2^{BC} (1^{B})	9±3 (1)	72±9^{B} (9^{AB})	55±3^{B} (10^{A})	24±6^{B} (3)	22±1^{B} (4)
	BU	49±21^{A} (2^{B})	20±2^{A} (1^{B})	26±2^{AI} (1^{BI})	12±2^{i} (1^{i})	229±47^{A} (7^{B})	153±13^{A} (6^{B})	135±19^{A} (5)	101±14^{A} (5)
TSP	SMaA	18±4^{B} (4^{A})	11±2^{B} (3^{A})	29±18^{A} (8)	14±7 (4^{A})	33±5^{D} (8)	30±1^{C} (9^{A})	17±5^{B} (4^{B})	17±2^{B} (5)
	LMiA	15±1^{Bi} (3^{AB})	16±1^{ABaI} (3^{A})	10±5^{B} (2)	8±4 (1^{AB})	53±5^{C} (11)	52±9^{B} (9^{A})	16±6^{B} (3^{B})	19±10^{B} (3)
	SMiA	18±2^{B} (3^{AB})	20±1^{Aa} (3^{A})	7±4^{B} (1)	9±4 (1^{AB})	70±2^{B} (11)	66±4^{B} (10^{A})	23±4^{B} (4^{B})	22±4^{B} (4)
	BU	31±4^{A} (2^{B})	24±10^{A} (1^{B})	18±7^{AB} (1)	15±3 (1^{B})	189±12^{A} (8^{I})	166±24^{A} (6^{Bi})	168±48^{A} (8^{A})	128±36^{A} (5)
BC	SMaA	16±4^{B} (4^{A})	6±0^{D} (2^{AB})	23±22^{A} (6)	6±3^{AB} (2^{A})	33±5^{BI} (9^{I})	23±2^{Ci} (7^{i})	20±8^{B} (5)	11±6^{B} (3^{AB})
	LMiA	15±1^{B} (3^{AB})	11±3^{Cab} (3^{A})	7±3^{A} (1)	5±1^{AB} (1^{AB})	53±6^{B} (11)	40±12^{BC} (10)	17±6^{B} (4)	10±8^{B} (2^{B})
	SMiA	18±2^{B} (3^{AB})	16±1^{Bab} (2^{AB})	9±3^{A} (1)	4±1^{B} (1^{AB})	71±3^{BI} (10)	58±2^{Bi} (9)	25±6^{B} (4)	18±9^{B} (3^{AB})
	BU	41±14^{A} (2^{B})	19±2^{A} (1^{B})	18±6^{A} (1)	13±9^{A} (1^{B})	208±45^{A} (7)	179±24^{A} (7)	145±46^{A} (7)	132±20^{A} (6^{A})
BC^{plus}	SMaA	16±3^{B} (4)	12±5^{AB} (3^{A})	17±11^{B} (4)	14±11 (4)	36±2^{C} (8)	29±9^{C} (8^{AB})	18±3^{B} (4)	12±1^{B} (3)
	LMiA	15±1^{B} (4)	12±1^{Bab} (3^{A})	8±6^{BC} (2)	6±3 (1)	51±5^{BC} (12)	37±3^{C} (9^{A})	21±5^{B} (5)	15±7^{B} (4)
	SMiA	17±2^{B} (2)	14±2^{ABb} (2^{AB})	6±1^{C} (1)	7±2 (1)	71±8^{B} (10)	55±11^{B} (9^{A})	23±3^{B} (3)	22±3^{B} (4)
	BU	40±22^{A} (2)	17±4^{A} (1^{B})	27±1^{A} (1)	14±7 (1)	210±40^{A} (8)	164±16^{A} (6^{B})	148±29^{A} (7)	117±40^{A} (5)

Table S4 (continued)

Treatment	Size fraction	NaOH-P_i		NaOH-P_o		H_2SO_4-P	
		mg kg^{-1} fraction (%)					
		Before start (2013)	2018	Before start (2013)	2018	Before start (2013)	2018
No-P	SMaA	107±26^{C} (24^{AB})	79±14^{Dab} (24^{AB})	202±96^{B} (44)	143±47^{B} (42)	55±12^{B} (13)	48±7^{B} (14^{B})
	LMiA	120±33^{C} (29^{A})	132±16^{Cab} (26^{AB})	95±47^{Bi} (23^{i})	190±27^{BI} (37^{I})	93±14^{B} (24)	113±9^{B} (22^{A})
	SMiA	196±21^{B} (26^{AB})	178±6^{B} (31^{A})	330±72^{B} (43)	190±68^{B} (32)	111±10^{B} (15^{i})	116±5^{B} (20^{AI})
	BU	534±15^{AI} (17^{Bi})	484±23^{Ai} (20^{BI})	1160±520^{A} (36)	844±383^{A} (33)	442±45^{A} (15)	498±101^{A} (20^{Aa})
TSP	SMaA	100±25^{D} (25^{AB})	95±4Da (27^{B})	148±28^{B} (36)	123±17^{B} (35)	56±3^{C} (14^{B})	59±7^{C} (17)
	LMiA	150±6^{C} (30^{A})	147±10^{Ca} (27^{B})	153±33^{B} (30)	191±30^{B} (35)	108±13^{B} (21^{A})	118±26^{B} (21)
	SMiA	210±8^{B} (32^{A})	208±10^{B} (33^{A})	200±75^{B} (30)	181±63^{B} (28)	123±19^{B} (19^{AB})	129±17^{B} (20)
	BU	514±24^{A} (21^{BI})	498±5^{A} (17^{Ci})	648±67^{Ai} (27^{i})	1132±152^{AI} (39^{I})	349±20^{Ai} (14^{AB})	468±47^{AI} (16^{b})
BC	SMaA	97±25^{D} (26^{AB})	64±10^{Db} (21)	131±15^{B} (35)	104±36^{B} (34)	51±8^{C} (14^{B})	93±56^{B} (30)
	LMiA	146±8^{C} (31^{A})	115±24^{Cab} (30)	128±53^{B} (26)	111±55^{B} (27)	106±15^{BC} (22^{A})	103±40^{B} (26)
	SMiA	208±7^{B} (29^{AB})	189±21^{B} (28)	263±103^{B} (36)	248±110^{B} (36)	116±14^{B} (17^{AB})	135±22^{B} (21)
	BU	518±30^{A} (19^{B})	516±34^{A} (21)	999±635^{A} (33)	704±209^{A} (28)	368±38^{A} (13^{B})	486±95^{A} (19^{ab})
BC^{plus}	SMaA	110±24^{C} (23)	78±11^{Cab} (21^{B})	219±79^{B} (45)	130±27^{B} (35)	61±5^{B} (13^{i})	95±14^{B} (26^{I})
	LMiA	123±37^{C} (28)	105±5^{Cb} (26^{A})	120±54^{B} (27)	126±11^{B} (32)	96±15^{B} (23)	97±15^{B} (24)
	SMiA	198±23^{B} (29)	181±23^{B} (29^{A})	267±114^{B} (37)	191±58^{B} (31)	117±19^{B} (17)	144±36^{B} (24)
	BU	530±9^{A} (20)	495±31^{A} (18^{B})	809±204^{A} (29)	1003±260^{A} (37)	424±71^{A} (15)	447±4^{A} (17^{b})

Table S4 (continued)

Treatment	Size fraction	P_i		P_o		P_i / P_o	
		mg kg^{-1} fraction (%)					
		Before start (2013)	2018	Before start (2013)	2018	Before start (2013)	2018
No-P	SMaA	212±35^{C} (49^{B})	160±25^{C} (48^{AB})	234±94^{B} (51^{A})	175±53^{B} (52^{AB})	1.0±0.2^{B}	0.9±0.2^{B}
	LMiA	280±26^{C} (70^{AI})	294±23^{B} (58^{ABi})	122±43^{Bi} (30^{Bi})	217±31^{BI} (42^{ABI})	2.4±0.7^{A}	1.4±0.2^{AB}
	SMiA	396±31^{B} (53^{AB})	364±5^{Bb} (63^{A})	362±76^{B} (47^{AB})	220±66^{B} (37^{B})	1.1±0.3^{B}	1.7±0.4^{A}
	BU	1255±97^{A} (41^{Bi})	1156±128^{A} (47^{BI})	1869±562^{AI} (59^{AI})	1339±420^{Ai} (53^{Ai})	0.7±0.2^{Bi}	0.9±0.2^{BI}
TSP	SMaA	208±29^{D} (52^{AB})	195±10^{D} (56^{A})	195±25^{B} (48^{AB})	154±8^{B} (44^{B})	1.1±0.2^{B}	1.3±0.1^{B}
	LMiA	326±13^{C} (65^{A})	334±40^{C} (60^{A})	180±42^{B} (35^{B})	218±31^{B} (40^{B})	1.9±0.4^{A}	1.6±0.3^{B}
	SMiA	420±20^{B} (65^{A})	424±14^{Ba} (67^{A})	230±75^{B} (35^{B})	212±56^{B} (33^{B})	1.9±0.6^{A}	2.1±0.5^{A}
	BU	1084±31^{A} (45^{B})	1156±33^{A} (40^{B})	1345±198^{A} (55^{A})	1717±95^{A} (60^{A})	0.8±0.1^{B}	0.7±0.0^{C}
BC	SMaA	197±29^{C} (53^{AB})	186±49^{C} (60)	175±10^{B} (47^{AB})	121±43^{B} (40)	1.1±0.1^{B}	1.8±1.1^{AB}
	LMiA	320±21^{B} (68^{A})	268±65^{BC} (69)	152±59^{B} (32^{B})	127±63^{B} (31)	2.3±0.7^{A}	2.3±0.6^{A}
	SMiA	414±12^{B} (59^{AB})	398±16^{Ba} (61)	297±107^{B} (41^{AB})	270±109^{B} (39)	1.5±0.7^{AB}	1.7±0.8^{AB}
	BU	1135±119^{A} (42^{B})	1201±147^{A} (48)	1692±708^{A} (58^{A})	1317±298^{A} (52)	0.7±0.2^{B}	0.9±0.1^{B}
BC^{plus}	SMaA	223±26^{C} (47^{ABi})	214±24^{C} (58^{AI})	254±76^{B} (53^{ABI})	156±24^{B} (42^{Bi})	0.9±0.1^{Bi}	1.4±0.1^{BI}
	LMiA	286±34^{C} (66^{A})	251±22^{C} (63^{A})	149±51^{B} (34^{B})	147±20^{B} (37^{B})	2.0±0.6^{A}	1.7±0.4^{AB}
	SMiA	402±39^{B} (58^{AB})	394±9^{Bab} (64^{A})	296±114^{B} (42^{AB})	220±59^{B} (36^{B})	1.5±0.7^{AB}	1.9±0.4^{A}
	BU	1204±120^{A} (44^{B})	1124±47^{A} (42^{B})	1521±193^{A} (56^{A})	1555±147^{A} (58^{A})	0.8±0.0^{B}	0.7±0.1^{C}

SMaA = small macroaggregate. LMiA = large microaggregate. SMiA = small microaggregate. BU = building units. TSP = triple superphosphate. BC = bone char. BC^{plus} = sulfur modified bone char. P_t = total P. P_i = total inorganic P. P_o = total organic P.

Significant differences between size fractions within a treatment in the same year were labeled with different capital letters; between four treatments within an aggregate size fraction in the same year were labeled with different lowercase letters; between years within a size fraction and a treatment were labeled with i or I, respectively. The value labelled with “I” was tested significantly higher than value labelled with “i”. Values were mean ± standard deviation (n = 3). Values in brackets were proportions of each P fraction to total P in each soil size fraction.

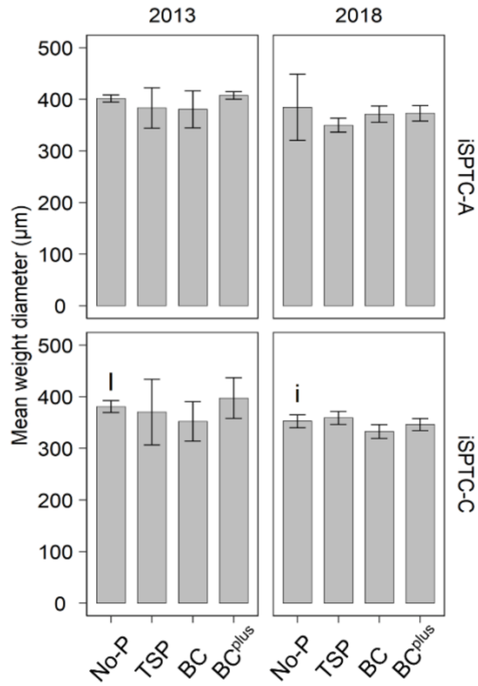

Figure S1. Effects of treatments (No phosphorus, No-P; triple superphosphate, TSP; bone char, BC; and sulfur modified bone char, BC^{plus}) on mean weight diameter (MWD, µm) in iSPTC-A and iSPTC-C soils. Significant differences between years within a size fraction and a treatment were labeled with i or I, respectively. The value labelled with "I" was tested significantly higher than value labelled with "i". n = 3.

Estimation of P loss during wet-sieving

We used 40.0 g bulk soil (< 2 mm) and 600 mL MilliQ water for the wet-sieving (two sieves stack: 250 and 53 μm) procedure. The suspensions with soil size fractions < 53 μm were centrifuged to get size fraction < 1 μm. Then the suspensions with size fraction < 1 μm were concentrated with tangential flow filtration (TFF). With TFF, the suspension volume was reduced to less than 10 mL. Hence, about 590 mL filtrates were discarded and resulted to H_2O-P loss. We did not measured the P concentration of filtrates of the studied samples, while we determined total P concentration of filtrates obtained with the same method of other soil samples and it was 0.10±0.03 mg P/L. If we use this value for estimation, then 0.059±0.018 mg P was lost. For 40.0 g bulk soil, the extracted H_2O-P mass ranged from 0.2 to 3.8 mg P. Hence, we roughly get that the lost P accounted for 1.6 to 29.5% of the extracted H_2O-P. Hence, in some cases, the P loss via wet-sieving should not be neglected.

Data for Figure 1

Aggregates	Year	P_level	Treatments	Proportion	stdev
SMaA	2013	A	No-P	30.908	0.302
LMiA	2013	A	No-P	29.335	2.777
SMiA	2013	A	No-P	35.092	3.022
BU	2013	A	No-P	1.409	0.493
SMaA	2018	A	No-P	29.725	5.672
LMiA	2018	A	No-P	26.014	1.194
SMiA	2018	A	No-P	39.554	5.431
BU	2018	A	No-P	1.068	0.094
SMaA	2018	C	No-P	26.600	0.993
LMiA	2018	C	No-P	27.822	1.215
SMiA	2018	C	No-P	41.311	1.377
BU	2018	C	No-P	1.156	0.074
SMaA	2013	C	No-P	29.092	1.260
LMiA	2013	C	No-P	28.679	2.310
SMiA	2013	C	No-P	37.090	2.274
BU	2013	C	No-P	1.205	0.044
SMaA	2018	A	TSP	25.908	1.176
LMiA	2018	A	TSP	31.729	1.131
SMiA	2018	A	TSP	38.068	0.878
BU	2018	A	TSP	0.919	0.094
SMaA	2013	A	TSP	29.149	3.359
LMiA	2013	A	TSP	30.079	1.758
SMiA	2013	A	TSP	36.045	4.109
BU	2013	A	TSP	1.345	0.264
SMaA	2018	C	TSP	27.016	1.242
LMiA	2018	C	TSP	29.233	2.118
SMiA	2018	C	TSP	39.470	2.249
BU	2018	C	TSP	1.200	0.131
SMaA	2013	C	TSP	28.146	5.856
LMiA	2013	C	TSP	28.487	2.207
SMiA	2013	C	TSP	38.731	5.401
BU	2013	C	TSP	1.359	0.450

SMaA	2018	A	BC	27.903	1.607
LMiA	2018	A	BC	30.972	1.452
SMiA	2018	A	BC	38.438	0.951
BU	2018	A	BC	1.195	0.104
SMaA	2013	A	BC	28.870	3.021
LMiA	2013	A	BC	30.418	2.021
SMiA	2013	A	BC	35.731	4.436
BU	2013	A	BC	1.442	0.197
SMaA	2018	C	BC	24.563	0.830
LMiA	2018	C	BC	29.597	3.248
SMiA	2018	C	BC	42.160	3.757
BU	2018	C	BC	1.165	0.643
SMaA	2013	C	BC	26.727	3.511
LMiA	2013	C	BC	27.008	1.094
SMiA	2013	C	BC	39.500	4.074
BU	2013	C	BC	1.455	0.309
SMaA	2018	A	BCplus	28.265	1.400
LMiA	2018	A	BCplus	29.437	0.278
SMiA	2018	A	BCplus	38.817	1.931
BU	2018	A	BCplus	1.334	0.125
SMaA	2013	A	BCplus	31.187	0.734
LMiA	2013	A	BCplus	30.955	0.224
SMiA	2013	A	BCplus	35.406	2.634
BU	2013	A	BCplus	1.313	0.514
SMaA	2018	C	BCplus	25.736	1.363
LMiA	2018	C	BCplus	30.003	2.754
SMiA	2018	C	BCplus	41.268	1.538
BU	2018	C	BCplus	0.842	0.163
SMaA	2013	C	BCplus	30.512	3.672
LMiA	2013	C	BCplus	29.317	1.453
SMiA	2013	C	BCplus	36.321	3.491
BU	2013	C	BCplus	1.110	0.193

Data for Figure 2

Aggregates	Year	P_level	Treatments	P proportion	stdev
SMaA	2013	A	No-P	25.453	2.114
LMiA	2013	A	No-P	24.506	3.061
SMiA	2013	A	No-P	45.140	2.472
BU	2013	A	No-P	4.901	1.955
SMaA	2018	A	No-P	18.749	4.073
LMiA	2018	A	No-P	24.290	1.060
SMiA	2018	A	No-P	52.556	5.748
BU	2018	A	No-P	4.405	0.737
SMaA	2013	C	No-P	23.179	5.504
LMiA	2013	C	No-P	20.778	3.852
SMiA	2013	C	No-P	50.447	2.676
BU	2013	C	No-P	5.595	1.280
SMaA	2018	C	No-P	17.952	4.353
LMiA	2018	C	No-P	28.582	3.038
SMiA	2018	C	No-P	48.594	6.955
BU	2018	C	No-P	4.871	0.967
SMaA	2013	A	TSP	20.974	2.797
LMiA	2013	A	TSP	23.249	2.217
SMiA	2013	A	TSP	50.825	2.080
BU	2013	A	TSP	4.952	1.025
SMaA	2018	A	TSP	20.500	5.745
LMiA	2018	A	TSP	32.867	0.841
SMiA	2018	A	TSP	43.203	5.079
BU	2018	A	TSP	3.430	0.553
SMaA	2013	C	TSP	21.564	7.329
LMiA	2013	C	TSP	26.746	1.214
SMiA	2013	C	TSP	46.940	7.116
BU	2013	C	TSP	4.750	1.182
SMaA	2018	C	TSP	17.655	1.613
LMiA	2018	C	TSP	30.099	2.468
SMiA	2018	C	TSP	46.800	3.977
BU	2018	C	TSP	5.447	0.661

SMaA	2013	A	BC	20.602	2.152
LMiA	2013	A	BC	25.609	2.314
SMiA	2013	A	BC	49.239	4.674
BU	2013	A	BC	4.550	0.357
SMaA	2018	A	BC	19.637	5.917
LMiA	2018	A	BC	26.295	2.592
SMiA	2018	A	BC	49.753	8.849
BU	2018	A	BC	4.315	0.765
SMaA	2013	C	BC	18.434	2.404
LMiA	2013	C	BC	23.791	4.586
SMiA	2013	C	BC	51.797	4.866
BU	2013	C	BC	5.977	0.985
SMaA	2018	C	BC	15.294	0.409
LMiA	2018	C	BC	23.586	7.546
SMiA	2018	C	BC	56.558	5.514
BU	2018	C	BC	4.562	2.215
SMaA	2013	A	BCplus	25.397	1.041
LMiA	2013	A	BCplus	23.375	2.305
SMiA	2013	A	BCplus	46.022	3.714
BU	2013	A	BCplus	5.205	1.999
SMaA	2018	A	BCplus	17.682	3.223
LMiA	2018	A	BCplus	28.324	2.329
SMiA	2018	A	BCplus	48.932	3.088
BU	2018	A	BCplus	5.062	0.932
SMaA	2013	C	BCplus	26.370	5.472
LMiA	2013	C	BCplus	23.261	5.219
SMiA	2013	C	BCplus	45.963	5.643
BU	2013	C	BCplus	4.407	0.948
SMaA	2018	C	BCplus	19.527	1.911
LMiA	2018	C	BCplus	24.530	2.526
SMiA	2018	C	BCplus	51.970	1.909
BU	2018	C	BCplus	3.973	1.214

Data for Figure 3

Aggregates	Treatments	P_level	Availability	P concentration (mg kg-1)	stdev
SMaA	No-P	A	Labile P	9.792	1.459
SMaA	No-P	A	Moderately labile P	44.379	6.804
SMaA	No-P	A	Stable P	16.063	6.019
LMiA	No-P	A	Labile P	11.558	1.052
LMiA	No-P	A	Moderately labile P	57.334	7.171
LMiA	No-P	A	Stable P	23.713	3.106
SMiA	No-P	A	Labile P	21.891	6.141
SMiA	No-P	A	Moderately labile P	143.804	32.183
SMiA	No-P	A	Stable P	37.780	12.336
BU	No-P	A	Labile P	1.775	0.389
BU	No-P	A	Moderately labile P	11.175	0.953
BU	No-P	A	Stable P	3.666	1.480
SMaA	TSP	A	Labile P	16.329	6.073
SMaA	TSP	A	Moderately labile P	43.332	15.514
SMaA	TSP	A	Stable P	22.920	17.298
LMiA	TSP	A	Labile P	18.723	3.235
LMiA	TSP	A	Moderately labile P	86.063	7.136
LMiA	TSP	A	Stable P	25.626	4.985
SMiA	TSP	A	Labile P	25.468	0.832
SMiA	TSP	A	Moderately labile P	105.100	13.455
SMiA	TSP	A	Stable P	39.907	10.370
BU	TSP	A	Labile P	2.257	0.138
BU	TSP	A	Moderately labile P	8.011	1.461
BU	TSP	A	Stable P	3.295	0.534
SMaA	BC	A	Labile P	8.708	0.868
SMaA	BC	A	Moderately labile P	43.407	13.493
SMaA	BC	A	Stable P	21.232	14.632
LMiA	BC	A	Labile P	11.660	0.883
LMiA	BC	A	Moderately labile P	65.019	12.598
LMiA	BC	A	Stable P	21.367	3.167
SMiA	BC	A	Labile P	16.952	0.471
SMiA	BC	A	Moderately labile P	126.164	31.062
SMiA	BC	A	Stable P	42.452	6.962
BU	BC	A	Labile P	1.812	0.295
BU	BC	A	Moderately labile P	10.147	3.675
BU	BC	A	Stable P	4.353	0.976
SMaA	BCplus	A	Labile P	9.402	1.980
SMaA	BCplus	A	Moderately labile P	43.767	5.181
SMaA	BCplus	A	Stable P	14.100	3.188
LMiA	BCplus	A	Labile P	13.154	4.158
LMiA	BCplus	A	Moderately labile P	68.583	17.083
LMiA	BCplus	A	Stable P	28.517	5.604

SMiA	BCplus	A	Labile P	22.869	7.264
SMiA	BCplus	A	Moderately labile P	121.415	29.629
SMiA	BCplus	A	Stable P	46.838	10.108
BU	BCplus	A	Labile P	2.496	0.734
BU	BCplus	A	Moderately labile P	12.730	4.077
BU	BCplus	A	Stable P	4.488	0.562
SMaA	No-P	C	Labile P	17.221	3.340
SMaA	No-P	C	Moderately labile P	59.434	17.488
SMaA	No-P	C	Stable P	12.885	2.408
LMiA	No-P	C	Labile P	21.458	2.207
LMiA	No-P	C	Moderately labile P	89.559	10.907
LMiA	No-P	C	Stable P	31.367	3.127
SMiA	No-P	C	Labile P	41.464	3.095
SMiA	No-P	C	Moderately labile P	152.343	30.682
SMiA	No-P	C	Stable P	48.057	3.205
BU	No-P	C	Labile P	3.308	0.092
BU	No-P	C	Moderately labile P	15.194	3.677
BU	No-P	C	Stable P	5.712	0.804
SMaA	TSP	C	Labile P	19.678	3.863
SMaA	TSP	C	Moderately labile P	58.841	2.586
SMaA	TSP	C	Stable P	15.880	2.508
LMiA	TSP	C	Labile P	27.845	2.674
LMiA	TSP	C	Moderately labile P	99.032	8.638
LMiA	TSP	C	Stable P	34.102	5.558
SMiA	TSP	C	Labile P	46.699	4.149
SMiA	TSP	C	Moderately labile P	154.030	34.115
SMiA	TSP	C	Stable P	51.059	8.270
BU	TSP	C	Labile P	3.944	0.282
BU	TSP	C	Moderately labile P	19.631	3.523
BU	TSP	C	Stable P	5.624	0.943
SMaA	BC	C	Labile P	11.325	1.202
SMaA	BC	C	Moderately labile P	41.174	10.033
SMaA	BC	C	Stable P	23.052	14.362
LMiA	BC	C	Labile P	19.416	3.483
LMiA	BC	C	Moderately labile P	67.012	23.959
LMiA	BC	C	Stable P	30.551	13.701
SMiA	BC	C	Labile P	40.508	7.207
SMiA	BC	C	Moderately labile P	181.312	41.404
SMiA	BC	C	Stable P	57.429	14.477
BU	BC	C	Labile P	3.821	1.927
BU	BC	C	Moderately labile P	13.172	5.910
BU	BC	C	Stable P	5.267	2.401
SMaA	BCplus	C	Labile P	17.489	5.316
SMaA	BCplus	C	Moderately labile P	53.558	10.022
SMaA	BCplus	C	Stable P	24.315	2.647

LMiA	BCplus	C	Labile P	21.025	2.552
LMiA	BCplus	C	Moderately labile P	69.165	4.133
LMiA	BCplus	C	Stable P	29.045	5.774
SMiA	BCplus	C	Labile P	40.653	5.979
SMiA	BCplus	C	Moderately labile P	153.416	32.919
SMiA	BCplus	C	Stable P	59.531	15.049
BU	BCplus	C	Labile P	2.571	0.130
BU	BCplus	C	Moderately labile P	12.849	4.434
BU	BCplus	C	Stable P	3.774	0.771